Coralline algal assemblages record Miocene sea-level changes in the South China Sea

Yinqiang Li [a], Kefu Yu [a,b,*], Lizeng Bian [a,c], Yeman Qin [a], Weihua Liao [a,d], Yang Yang [a], Yifang Ma [a]

[a] Guangxi Laboratory on the Study owef Coral Reefs in the South China Sea, Coral Reef Research Center of China, School of Marine Sciences, Guangxi University, Nanning 530004, China
[b] Southern Marine Sciences and Engineering Guangdong Laboratory (Zhuhai), Zhuhai 519000, China
[c] School of Earth Sciences and Engineering, Nanjing University, Nanjing 210093, China
[d] Nanjing Institute of Geology and Palaeontology, Chinese Academy of Sciences, Nanjing 210008, China

ARTICLE INFO

ABSTRACT

We have previously shown that the coralline algal assemblages (CAAs) of the South China Sea may indicate post-Pliocene paleo-water depth changes; however, the pre-Pliocene coralline algal compositions and related sea-level significance remain to be elucidated. In the present study, we explore the Miocene coralline algal compositions and their role in recording the sea level, and show the distribution, classification, type, abundance, and diversity of Miocene coralline algae from 213 petrologic thin sections using a coral-reef carbonate sequence from the northern South China Sea. The diversity and abundance of coralline algae in the early and late Miocene are higher than those in the middle Miocene. Eleven genera were identified and grouped into seven CAAs, showing a water depth range from <5 m to >25 m. At 18.67–17.98 Ma, the coral reef was in a stagnation/drowning stage, with rising sea levels exceeding the development of the coral reef. At 17.98–16.78 Ma, the coral reef was in a rapid development during a rapid rise in sea level. Additionally, at 16.78–14.79 Ma, low coralline algal abundance was observed, and the corals were sporadically distributed at a relatively stable sedimentation rate, suggesting a decline in coral reef development. At 14.79–10 Ma, the coral reef development was remarkably slow or stagnant. Furthermore, at 10–5.3 Ma, the coral reefs developed slowly, indicating a gradual rise in the sea level. The sea-level changes indicated by coral reef development are consistent with the long-term global sea-level changes, indicating that the composition and assemblage of Miocene coralline algae can be used to accurately relay the sea-level history.

1. Introduction

Shallow-water carbonate deposits comprising fossil reefs can record various geological events such as sea-level fluctuations, paleoclimatic conditions, and paleoceanographic changes (Abbey et al., 2011; Braga and Martín, 1996; Coletti and Basso, 2020; Coletti et al., 2018; Coletti et al., 2019; Hallmann et al., 2013; Iryu et al., 2010; Kershaw et al., 2005). These deposits play a crucial role in recording sea-level fluctuations or environmental changes such as light attenuation or variation in hydrodynamic energy (Abbey et al., 2011; Adey and Macintyre, 1973; Aguirre et al., 2000; Bassi et al., 2009; Braga and Bassi, 2012; Li et al., 2021; Wanamaker et al., 2011). Coralline algae preserved in in situ reefs

can help to reconstruct the paleoecology and the paleoenvironment (Braithwaite, 2016). The South China Sea (SCS) provides an excellent archive for the study of sea-level history by analyzing shallow-water deposits as it is one of the most important regions for global carbonate production and coral reef development since the Miocene period (Wang, 2009). Moreover, previous studies reported that the paleo-water depths recorded by coralline algae in the SCS are indicative of a long-term deepening trend starting from the Pliocene (Li et al., 2021). However, geographical distribution peculiarities, along with insufficient information on the global bathymetric distribution of coralline algae, as well as their complex taxonomic history hamper the possibility of using coralline algae paleoenvironmental reconstructions (Coletti and Basso,

---

2020). Furthermore, studies on the environmental records of coralline algal assemblages (CAAs) in Miocene reefs are limited due to incomplete preservation and the coarse chronological frameworks of shallow water carbonates. Thus, it is of utmost importance to understand the evolution and paleoecology of CAAs in coral reefs for deeper insights into regional paleobiogeography, paleoclimate, and paleoenvironment.

Water depth/eustasy is one of the most important variables in the reconstruction of the shallow-water paleoenvironments (Bard et al., 1996; Coletti et al., 2018; Iryu et al., 2010; Li et al., 2021; Perrin et al., 1995; Wu et al., 2019). Paleobathymetric studies are based on the distribution of biological assemblages and sedimentary indicators (e.g., few well-preserved reef flat complexes) (Bard et al., 1996; Coletti et al., 2018; Iryu et al., 2010; Li et al., 2021; Perrin et al., 1995; Wu et al., 2019). Moreover, the distribution of calcified red algae is primarily controlled by light availability and hydrodynamic energy (Steneck, 1986; Adey and Macintyre, 1973; Adey, 1986; Bosence, 1991; Bosence, 1983; Sane et al., 2016), wherein light availability decreases with increasing water depth. Furthermore, the sorting and size of sediments formed by coralline algae are also controlled by hydrodynamic energy, which decreases with an increase in water depth (Sane et al., 2016). However, the reliability of reconstructed bathymetric curves can vary based on this model, making it necessary to accurately identify the indicator species in the coralline algal community and relate them to the characteristics of the environmental habitat (Cabioch et al., 1999b).

Considering the present coralline algal distribution, Quaternary sea-level changes have been reconstructed based on the drilling of several scientific cores (Cabioch et al., 1999b; Iryu et al., 2010; Li et al., 2021). Thus, it is important to understand the response of the coralline algal community to environmental changes. In particular, time-series changes in deep- (reef drowning) and shallow-water assemblages (reef regeneration) should be identified to better understand the sea-level changes. Increased glacial activity in the northern hemisphere since the Pliocene expanded the polar ice volume and reduced sea levels over a long period (Miller et al., 2005). Furthermore, long-term periodic eustasy since the Pliocene and vast changes in paleoceanographic conditions affected the evolution of tropical shallow-water carbonate systems (Wu et al., 2019).
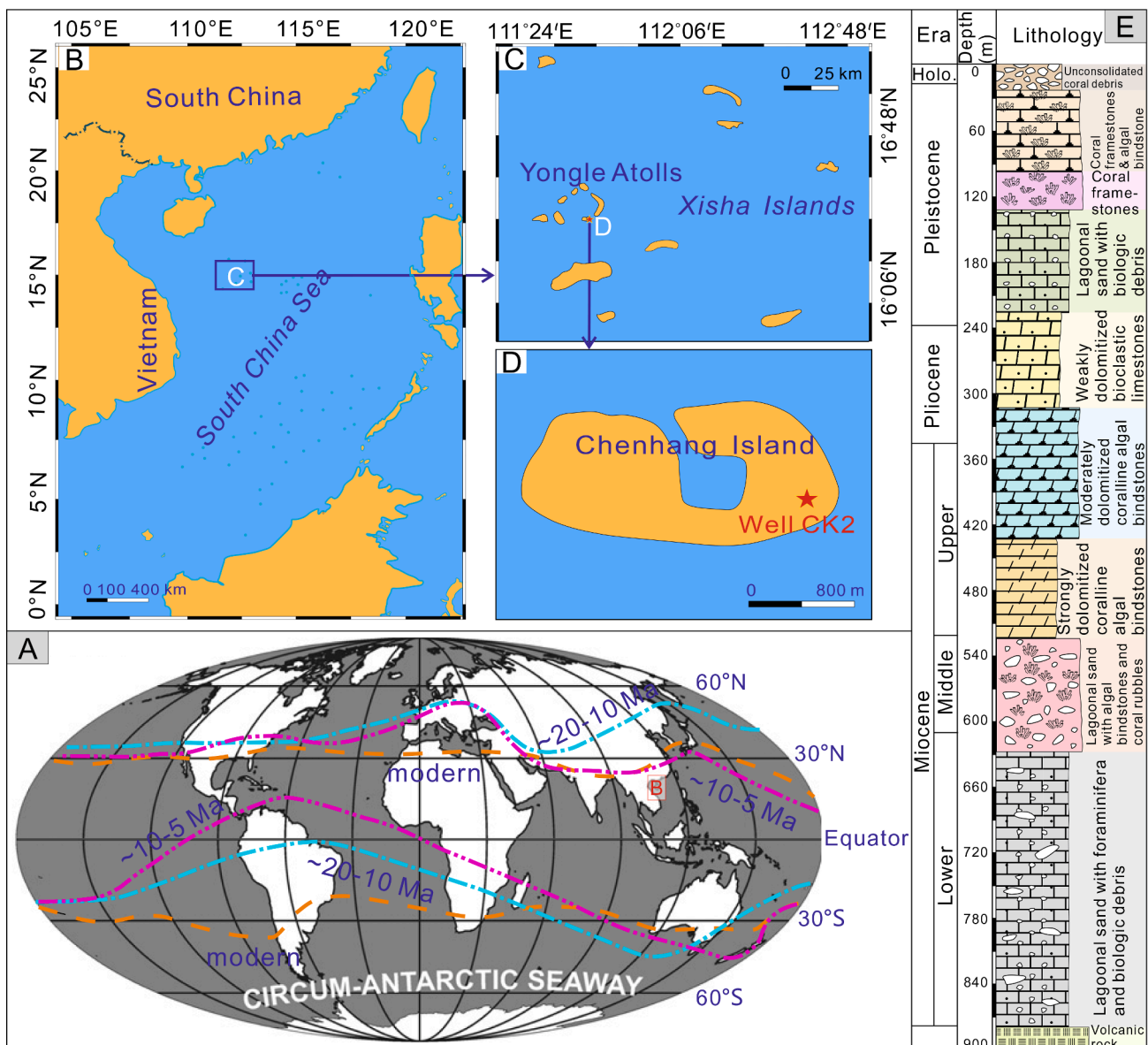
Fig. 1. Location and stratigraphic profile of Well CK2 on Chenhang Island in the northern South China Sea (SCS) including **A** the distribution range of coral reefs, at present and during the Miocene (modified from Perrin (2002)). The geography of the world as reported by Hay (2011). **B**, **C**, and **D** refer to the location of the well. **E** Lithology and stratigraphic chronology as reported by Fan et al. (2020).

In the SCS, *Mesophyllum* assemblage, indicative of deep water, was replaced by *Lithoporella-Lithophyllum* assemblage, thereby signifying relatively shallow-water settings and supporting a decrease sea level (Li et al., 2021).

Coral reef ecosystems can provide strong evidence for long-term periodic fluctuations in sea level, thereby revealing consistent periodic records with global changes (Braithwaite, 2016). The Miocene is considered as a key period in the Cenozoic cooling history (Steinthorsdottir et al., 2020; Herbert et al., 2016), wherein the climatic shift caused significant changes in plant diversity (Bradshaw, 2021). The transition of global dominated carbonate assemblage from coral into rhodolith during the Burdigalian to early Tortonian may be associated with the Miocene global change (Halfar and Mutti, 2005). Furthermore, changes of calcification rates and bathymetric zonation are attributed to the coevolution of corals and *Symbiodinium* zooxanthellae; parallelly with global cooling, at least on a regional scale, geochemical changes support the extensive aragonite precipitation during the late Miocene (Pomar and Hallock, 2007). Nevertheless, the number and the belt with latitudinal extension of coral reefs during the Miocene had increased (excluding the Mediterranean area) (Fig. 1A; Perrin, 2002; Perrin and Bosellini, 2012). These results were also verified during the development of coral reefs in the SCS (Fan et al., 2020; Shao et al., 2017a, 2017b). The results of $\delta^{18}O$ and Mg/Ca records of the Pacific benthic foraminifera showed that the ice storage was limited during the early Miocene, suggesting a small sea-level oscillation. The sea-level changes were small (< 20 m) during the Miocene climate optimum (MCO), relatively greatly (~50 m fall) at the end of the expansion of the Antarctic ice sheet (13.8 Ma), while kept stable from late middle Miocene to late Miocene (Miller et al., 2020). This continuous rise or fall in the sea level can predict events such as coral reef drowning or exposure. Moreover, algal ridges (Steneck et al., 1997), trottoirs (Adey, 1986), algal frameworks (Rasser and Piller, 2004), and algal cup reefs (Ginsburg and Schroeder, 2010) were specifically formed by coralline algae in response to the sea-level changes during coral reef development.

Coral reefs in SCS were initially observed at approximately 20 Ma (Fan et al., 2020) widely developed in the middle Miocene (Ma et al., 2011), and less developed during the late Miocene (Shao et al., 2017a, 2017b); additionally, they occupied an area equivalent in size to that of the Great Barrier Reef (Yu and Zhao, 2009). Herein, we studied the sea-level history of the Miocene by analyzing the succession of CAAs during different geological intervals based on the composition and assemblages of Miocene coralline algae from Well CK2 (Fig. 1D) drilled in the north of SCS. Furthermore, we identified and discussed the indicators of Miocene coral reef development and sea-level changes in SCS to evaluate the accuracy of sea-level curves reconstructed regionally using coralline algae. These algal assemblages provide regional information that can be used to reconstruct long-term global sea-level changes.

2. Materials and methods

2.1. Study area

The SCS, the largest marginal sea of the western Pacific Ocean and is located in a semi-enclosed environment (Fig. 1B), is developed due to rapid seafloor expansion during the Cenozoic, and has been recognized as an important area for carbonate platform development since the Miocene (Yu and Zhao, 2009). The well-known Xisha Islands (Paracel Islands) (Fig. 1C), consisting of over 40 sandbanks, islets, and reefs, are located in the northern SCS, and can be divided into the Xuande and Yongle atolls (Xu et al., 2010). These islands, with elevations of 2–8 m, primarily consist of sand, coral gravel, mollusks, benthic foraminifera, and calcareous algal debris (Jian et al., 1997). Data collected by meteorological stations in the region indicate an annual mean temperature of 26–27 °C, which is highly suitable temperature for coral reef development (Xu et al., 2010). At 15.5–10.5 Ma, the average tectonic subsidence rate was relatively lower in the Xisha Islands; however, between 10.5

and 5.5 Ma, the subsidence rate increased resulting in the gradual drowning of the carbonate platform over this period (Wu et al., 2018).

Several coral reef scientific drilling projects (Wells Xiyong 1, Xichen 1, Xichen2, Xishi 1, Xike1, and CK2) have been conducted in the Xisha Islands region over the past 50 years. These projects have provided essential data on the biostratigraphy, petrology, and palaeontology of carbonate platforms in this region; however, the development of reefs and their relationship with sea-level changes as indicated by CAAs are rarely investigated and discussed owing to the coarse stratigraphic frameworks and the poor core recovery rates.

2.2. Core collection and logging

Well CK2 (16°26′56″ N, 111°00′54″ E) is related to a major, kilometer-scale, scientific drilling project. It was drilled on Chenhang Island in 2013 (Fig. 1D), reaching a depth of 928.75 m (Fig. 1E) and an average core recovery of approximately 70%. The well consists of reef carbonates (0–873.55 m) as well as volcanic basement (873.55–928.75 m). The age model was constructed using strontium isotope ratio dating and magnetostratigraphy as reported by Fan et al. (2020) (Fig. 2). Thus, the investigated section from 873.55 m (19.6 Ma) to 344 m (5.3 Ma) could be identified as of the Miocene epoch; wherein 611 m and 524 m representing the boundaries of the early/middle Miocene and middle/late Miocene, respectively. These findings revealed a relatively high sedimentation rate during the early Miocene (Fig. 3), and a relatively low rate during the middle and late Miocene (Fan et al., 2020). Furthermore, the highest sedimentation rate is 428.57 m/Myr at 17.51 Ma (761 m), whereas the lowest is 2.12 m/Myr at 12.55 Ma (526 m). Miocene reef carbonates mainly consist of dolomite (late Miocene) and calcite (early and middle Miocene) (Fig. 2; Fan et al., 2020). Nine petrographic units have been identified based on the petrological characteristics of the drilling core; among which four units of Miocene were investigated in the present study (Fig. 1E). Based on the characteristics of Miocene lithological features (Wang et al., 2018), the three unconformities were identified at 364 m (6.04 Ma), 434.5 m (8.49 Ma), and 519 m (10.16 Ma). Among these, 364 m is representative of isabelline ferrous staining; 434.5 m characterize a change from tan/isabelline dolostones to white/offwhite; 519 m is characteristic of a change in lithology from white/offwhite limetones to the tan/isabelline dolostones.

Data on thin sections, core slab, and detailed visual descriptions of archived core halves were collected and analyzed to evaluate the changes in Miocene sea level based on the characteristics and variations of CAAs. The thick Miocene carbonate succession of approximately 530 m of Well CK2 was sampled every 3 m; moreover, additional samples were collected in coralline algae rich intervals, resulting in 168 and 45 samples, respectively. In total, 203 standard petrologic thin sections (ca. 2 × 3 cm) were prepared using conventional methods from the 213 collected samples. All thin sections are housed at the Coral Reef Research Center of China at Guangxi University.

Algae were identified under a polarizing microscope at the Coral Reef Research Center of China, Guangxi University. Furthermore, we investigated coralline algal abundance and diversity using the calculations proposed by Li et al. (2021), depicting the quantitative percentage and number of coralline algal genera in each thin section, respectively. Coralline algae were considered dominant if they accounted for more than 50% of a thin section. The morphological characteristics of coralline algae were consistent to those reported by Woelkerling et al. (1993). As coral abundance is semi-quantitative, we used the divisions of "rare/absent," "present," and "abundant" (Li et al., 2021). In addition, we used the following criteria from Camoin et al. (1997), Camoin et al. (2004), Webb et al. (2016), and Webster (2003) to distinguish the in situ coral or allochthonous rubble: 1) ensuring that fossilized communities are appropriately oriented, 2) understanding the orientation of geopetal surfaces, 3) considering coralline algal encrustation of coral colonies, and 4) the existence of a contact relationship between macroscopic
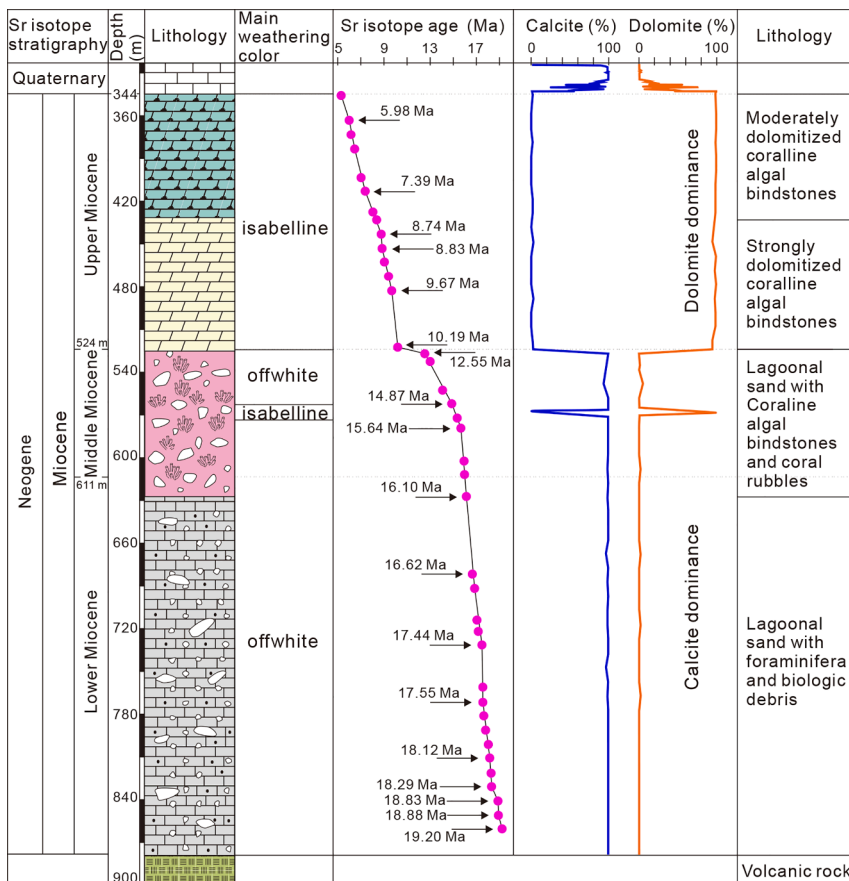
Fig. 2. Lithology and summary of primary weathering color, chronostratigraphy, and petrology. The chronostratigraphy and contents of calcite and dolomite in the investigated section are consistent with those observed by Fan et al. (2020). Dolomite is the dominant type of carbonate in the late Miocene with an isabelline primary weathering color, whereas carbonate is characteristic of calcite during early and middle Miocene, with an off-white primary weathering color. (For interpretation of the references to color in this figure legend, the reader is referred to the web version of this article.)

attached area and the underlying matrix. Moreover, carbonate rocks were classified according to Embry and Klovan (1971) classification. Considering the major boundary of 16.31 Ma, we divided the investigated sections into two important sedimentary units with 11 subunits based on the distribution of CAAs (Fig. 4). The quantitative primary data of coralline algal percentage are presented in the supplementary materials.

2.3. Fossil identification

Although coralline algae have been identified for 200 years since their inception as a phyto-group, they have a complex taxonomic history. Since the 1980s, the higher-level taxonomy of coralline algae has changed, resulting in different taxonomic frameworks. Thus, it is impossible to compare the datasets of water depth distribution generated under different classification frameworks (Coletti and Basso, 2020). To address these issues, we simplified the recent taxonomic schemes down to three coralline algal orders based on the molecular genetic data and morphological characteristics that can be identified in the geological record. The orders Corallinales and Hapalidiales are characterized by uniporate and multiporate conceptacles, respectively (Rösler et al., 2016; Nelson et al., 2015), whereas the order Sporolithales typically includes sporangi grouped in sori (Le Gall et al., 2009). Overall, this higher-level classification of coralline algae is supported by morphological evidences (Braga et al., 1993; Braga and Aguirre, 1995; Woelkerling, 1988; Coletti et al., 2018; Coletti and Basso, 2020) and genetic evidences (Harvey et al., 2003; Le Gall et al., 2009; Nelson et al., 2015; Rösler et al., 2016). Based on the identification approach used by Coletti and Basso (2020), Coletti et al. (2018), and Li et al. (2021), we identified the coralline algal groups in thin sections at the generic level or higher. The taxonomic scheme of corals is based on the taxonomic criteria (Humblet et al., 2015; Veron, 2000; Wallace, 1999). We used the scheme

only at the genus level due to diagenesis in present study. Furthermore, the terms of the developmental model of coral reef proposed by Macintyre and Neumann (2011) and Cabioch et al. (1999b), including "Keep-up", "Catch-up", and "Give-Up", were followed herein.

3. Results

Numerous shallow marine organisms (primarily coralline algae, corals, and foraminifera) were found in the investigated section of Well CK2. This section is dominated by reefal limestone, which well preserved the primary archives on the geological record. Coralline algae were abundantly present in the Miocene reef carbonates in the studied section of Well CK2 and were developed over corals or interdeveloped with corals and other encrusting organisms. In addition, to growing over the surfaces of corals, coralline algae also developed crusts over bioclastic gravels. In the studied core, 11 genera of coralline red algae were identified; however, their distribution and percentage differed across intervals. The types of coralline algae across the sites dominated by hydrodynamic energy were nonidentical. Descriptions of the facies and of the assemblages of each unit/subunit are summarized (Table 1) in the following subsections.

3.1. Unit A, 19.6-16.31 Ma, the first sedimentary cycle

3.1.1. Subunit a

Subunit *a* extends from 873.55 to 838.05 m (19.6–18.67 Ma) and is primarily composed of coralline algal packstones and coral framestones. Thin sections and lithological analyses indicated that the skeletal assemblage in this interval primarily consists of coralline algae and corals, constituting a coralline algal and coral facies. Larger benthic foraminifera (LBF) (Fig. 5I) and bryozoans (Fig. 5G) are distributed sporadically, whereas planktonic foraminifera are absent.
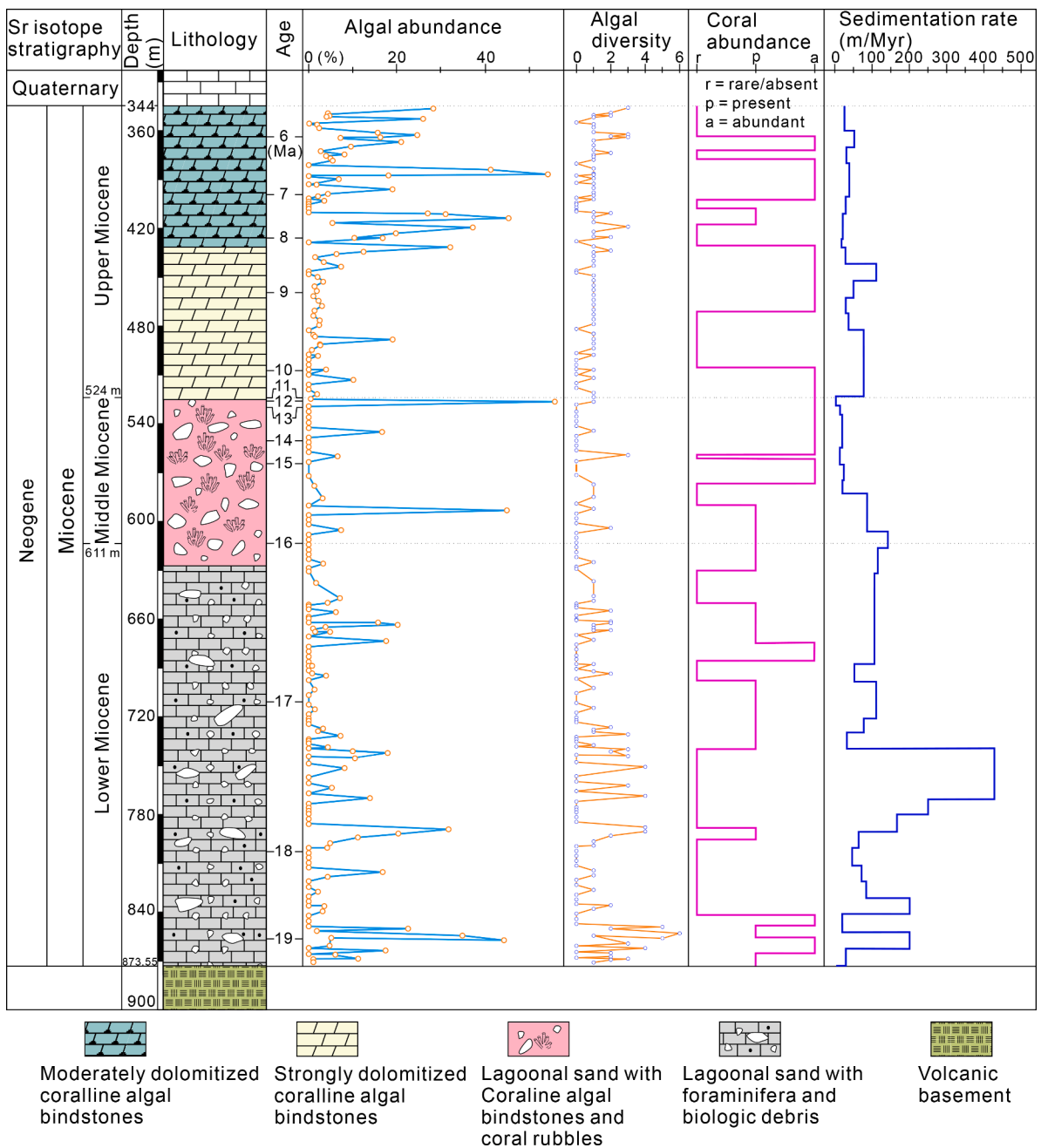
Fig. 3. Curves of coralline algal abundance, coralline algal diversity, coral abundance, and sedimentation rate obtained from Well CK2. Coralline algal abundance represents the area percentage in each thin section, and diversity represents the number of genera in the thin section corresponding to the coralline algal abundance. Estimated methods and significance of coral abundance were followed according to Li et al. (2021), whereas sedimentation rates were estimated using the methodology by Fan et al. (2020).

The analyses of 20 thin sections from this subunit indicate a coralline algal abundance ranging from 0 to 44.4%, averaging 8.3%, with the number of coralline algal genera ranging from 0 to 4, averaging 2 (Fig. 3). Articulated coralline algae (Fig. 5H) are richly distributed in packstones of the basal part of this subunit. In the upper part of the subunit, the algae exist within the framestone formed by corals. The coralline algal assemblage, CAA1, includes *Corallina* (Fig. 6E), *Jania*, *Hydrolitnon*, and *Lithoporella* (Fig. 6J). The encrusting genus *Mesophyllum* of the order Hapalidiales, *Neogoniolithon* (Fig. 6A), and *Lithophyllum* (Fig. 6H) were also observed in the thin sections (Fig. 4).

The coral abundance ranges from present to abundant except for interval 838.05–842.38 m, where they are absent (Fig. 3). Massive forms of *Astreopora* corals represent the main growth forms, followed by

branching *Acropora*, and encrusting *Montipora*.

3.1.2. Subunit b

Subunit *b* (838.05–801.15 m, 18.67–17.98 Ma) primarily consists of LBF rudstone and bioclastic packstones. Thin sections and lithology revealed that the skeletal assemblage mainly consists of LBF and coralline algae.

The analyses of 14 thin sections from this area show that the coralline algal abundance range from 0 to 16.9%, averaging ~2% (Fig. 3). The primary observed assemblage type of coralline algae is nongeniculate. The coralline algal diversity is relatively low, and the only genus of the assemblage (CAA2) is *Mesophyllum* (Fig. 4). Corals were not observed in this subunit (Fig. 3).
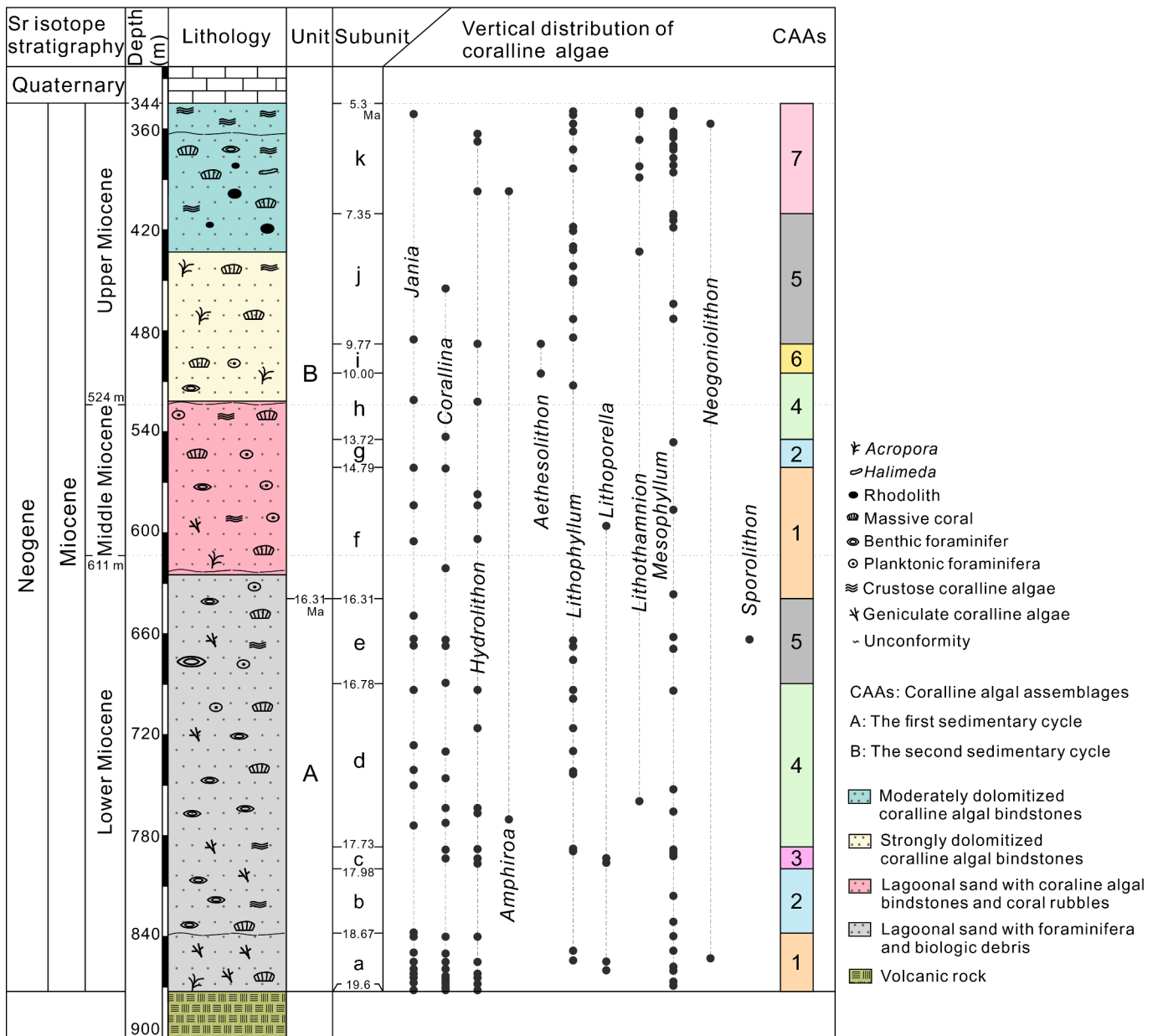
Fig. 4. Schematic logs of Well CK2 depicting variations in coralline algal assemblages (CAAs) and the vertical distribution of coralline algae. Each CAA is represented by a histogram of different colors. The age/Sr isotope stratigraphy is evaluated by the actual measurement calculated using values related to the strontium isotope and using the interpolation method suggested by Fan et al. (2020).

3.1.3. Subunit c

Subunit *c* (801.15–789.85 m; 17.98–17.73 Ma) is characterized by LBF packstones and coralline algal bindstones growing over the basement. Thin sections and lithology revealed that the main skeletal assemblage mainly consists of LBF and coralline algae. Moreover, planktonic foraminifera and corals occur sporadically in this interval.

The analyses of four thin sections from this area show coralline algal abundance ranging from 4.8 to 31.7%, with an average of approximately 17%, and genus diversity ranges from 1 to 5, with an average of 3 (Fig. 3). The type of coralline algae is mainly non-geniculate, with limited geniculate coralline algae. The common coralline algal genera include *Mesophyllum*, *Lithoporella*, *Lithophyllum*, *Hydrolithon*, and *Corallina*. Among them, *Hydrolithon* is the most abundant, followed by *Lithoporella* and *Lithophyllum*. They constitute the *Lithoporella-Lithophyllum-Hydrolithon* assemblage (CAA3) (Fig. 4). Only two corals genera occur in this subunit, *Turbinaria* and *Porites*.

3.1.4. Subunit d

Subunit *d* is approximately 100 m thick and goes from 789.85 to 689.07 m (17.73–16.78 Ma) and is overlaid with subunit *c*. From 789.85 to 740.07 m the interval is dominated by LBF and coralline algal packstones; from 740.07 to 689.07 m by bioclastic wackestones (Fig. 7E). Thin sections and lithology indicated coralline algae and foraminifera (mainly *Amphistegina* and *Heterostegina*) as the main components of the skeletal assemblages, with corals occurring as minor components (Fig. 5F).

The analyses of 39 thin sections indicate a coralline algal abundance ranging from 0 to 14%, with an average of 2.4%, and the genus diversity ranging from 0 to 4, with an average of 1 (Fig. 3). The assemblage comprises both non-geniculate and geniculate coralline algae, with the most common genera represented by *Lithophyllum*, *Hydrolithon*, *Jania*, and *Corallina*. Furthermore, the minor genera included *Mesophyllum*, *Lithothamnion* (Fig. 6I), and *Amphiroa*. The genera *Corallina*, *Jania*,

Table 1

Summary and description of all subunits obtained from Well CK2 including coralline algal assemblages (CAAs), facies, limestone classification, algal abundance, algal diversity, algal types, common algal genera, coral abundance, and water-depth range.

Subunits	CAAs/ thickness	Facies	Embry and Klovan (1971) classification	Algal abundance (average)	Algal diversity	Algal types	Common algal genera	Coral abundance	Water-depth range
Subunit *a*	CAA1/ 35.5 m	Coralline algal and coral	Packstone to framestone	0 to 44.4% (8.3%)	Moderate	Articulated, non-geniculate	*Corallina*, *Jania*, *Hydrolitnon*, and *Lithoporella*	Present to abundant	<5 m
Subunit *b*	CAA2/ 36.9 m	Coralline algal and foraminifera	Rudstone to packstone	0 to 16.9% (~2%)	Low	Non-geniculate	*Mesophyllum*	Absent	15–25 m
Subunit *c*	CAA3/ 11.3 m	Coralline algal and foraminifera	Packstone to bindstone	4.8 to 31.7% (~17%)	High	Non-geniculate, articulated	*Mesophyllum*, *Lithoporella*, *Lithophyllum*, *Hydrolithon*, and *Corallina*	Present	~10 m
Subunit *d*	CAA4/ ~100 m	Coralline algal and foraminifera	Packstone to wackstone	0 to 14% (2.4%)	Low	Non-geniculate, articulated	*Lithophyllum*, *Hydrolithon*, *Jania*, and *Corallina*.	Absent to present	<10 m
Subunit *e*	CAA5/ ~51 m	Coralline algal, coral and foraminifera	Packstone	0 to 20.2% (3.8%)	Low	Non-geniculate, articulated	*Lithophyllum* and *Mesophyllum*	Absent-present-abundant	15–20 m
Subunit *f*	CAA1/ ~78 m	Coralline algal and foraminifera	Packstone to bindstone and grainstone	0 to 45% (~3.3%)	Low	Non-geniculate, articulated	*Hydrolithon*, *Jania*, *Corallina*, and *Lithoporella*	Absent-present-abundant	<5 m
Subunit *g*	CAA2/ ~15 m	Foraminifera and coral	Packstone and framestone	0 to 16.8% (3.4%)	Low	Non-geniculate	*Mesophyllum*	Absent to abundant	15–25 m
Subunit *h*	CAA4/ 38.9 m	Corals and coralline algal	Framestone to bindstone	0 to 55.9% (5.8%)	Low	Non-geniculate, articulated	*Lithophyllum*, *Jania*, and *Hydrolithon*	Abundant	<10 m
Subunit *i*	CAA6/ 16.7 m	Coralline algal and corals	Bindstone	0 to 18% (3%)	Moderate	Non-geniculate	*Aethesolithon* and *Hydrolithon*	Abundant	<5 m
Subunit *j*	CAA5/ 79.4 m	Coralline algal and corals	Wackstone	0 to 45.4% (9.1%)	Moderate	Non-geniculate, articulated	*Mesophyllum* and *Lithophyllum*	Rare to abundant	15–20 m
Subunit *k*	CAA7/ 66 m	Coralline algal and corals	Wackstone to bindstone and framestone	0 to 54.4% (~9.3%)	High	Non-geniculate, articulated	*Mesophyllum*, *Lithothamnion*, and *Lithophyllum*	Absent to abundant	>20 m

Hydrolithon, and *Lithophyllum* dominate the assemblage and characterize the CAA4.

Corals are rare/absent in the basal part of this subunit. Notably, *Platygyra* coral was found in the core layers nearly 50 m thick (789.85–740.42 m) interval. Corals in the top interval include massive assemblages of *Platygyra*, *Astreopora*, *Porites*, and *Dipsastraea* (Fig. 3).

3.1.5. Subunit e

Subunit *e* is approximately 50 m thick (689.07–637.92 m, 16.78–16.31 Ma) and primarily consists of packstones. From 689.07 m to 668.07 m the interval is dominated by bioclastic packstones, accompanied by a small amount of coralline algal bindstones and wackstones. Apart from few grainstones, the interval (668.07–637.92 m) mainly consists of LBF packstones. Thin sections and lithology showed that the skeletal assemblage mainly comprises coralline algae, corals, and LBF (Fig. 5D). Planktonic foraminifera and large miliolids (Fig. 5E) are distributed sporadically in this subunit.

The analyses of 22 thin sections from this area revealed that coralline algal abundance ranges from 0 to 20.2%, averaging 3.8%, and genus diversity ranges from 0 to 4, with an average of 1 (Fig. 3). The assemblages comprise both non-geniculate and geniculate coralline algae. Furthermore, the for-algaliths formed by crustose coralline algae (CCA) and encrusting foraminifera occurs in this subunit (Fig. 7B), with *Lithophyllum* and *Mesophyllum* as the most common coralline algal genera (Fig. 6G and D, respectively), whereas *Jania* and *Corallina* are present as fragments. *Sporolithon* (Fig. 6F) only appears sporadically in this subunit. Therefore, CAA5 is dominated by *Lithophyllum* and *Mesophyllum* (Fig. 4).

Furthermore, the corals were abundantly found at 689.07–674.04 m, present at 674.04–650.04 m, and absent at 650.04–637.92 m (Fig. 3).

3.2. Unit B, 16.31-5.3 Ma, the second sedimentary cycle

3.2.1. Subunit f

Subunit *f* is approximately 100 m thick (637.92–560.07 m, 16.31–14.79 Ma) and mainly consists of LBF packstones. This subunit also include includes coralline algal bindstones and LBF grainstones in the basal part. The skeletal assemblage primarily consists of coralline algae, LBF, and corals, with planktonic foraminifera occurring as a minor component.

The analyses of 22 sections indicated that the coralline algal abundance ranges from 0 to 45%, averaging ~3.3% and genus diversity ranges from 0 to 3, with an average of 1 (Fig. 3). The coralline algae include both non-geniculated and geniculated forms. *Hydrolithon*, *Jania*, *Corallina*, and *Lithoporella* represent the most common coralline algal genera, while *Mesophyllum* and unidentified coralline algae are sporadically distributed in this subunit. Overall, CAA1 dominates the assemblage.

In the basal part (637.92–576.7 m), coral abundance ranges from absent to present, and coral assemblage mainly consist of branching *Acropora*, massive *Astreopora*, and *Platygyra*, and *Astrhelia*. Between 576.7 and 560.07 m, corals are abundant (Fig. 3).

3.2.2. Subunit g

Subunit *g* is 15 m thick (560.07–545 m; 14.79–13.72 Ma) and consists mostly of LBF packstones associated with sporadic massive coral framestones. Foraminifera and corals are the main components, and coralline algae occur as a minor component.

The analyses of five thin sections from this area indicate a coralline algal abundance ranging from 0 to 16.8%, with an average of 3.4%. The coralline algal diversity is low and the only genus identified is *Mesophyllum* (Fig. 3). Coralline algal genus in this subunit is single and comprise non-geniculated. Overall, *Mesophyllum* dominates the CAA2 (Fig. 4).

Coral abundance ranges from absent in the basal part of the subunit (560.07–555.74 m) to abundant in the upper section (555.74–545 m) (Fig. 3).

3.2.3. Subunit h

Subunit *h* is approximately 40 m thick (545–506.1 m; 13.72–10 Ma) and mainly consists of dolomitized coral framestones associated with a coralline algal bindstones. Coralline algae and corals dominate the
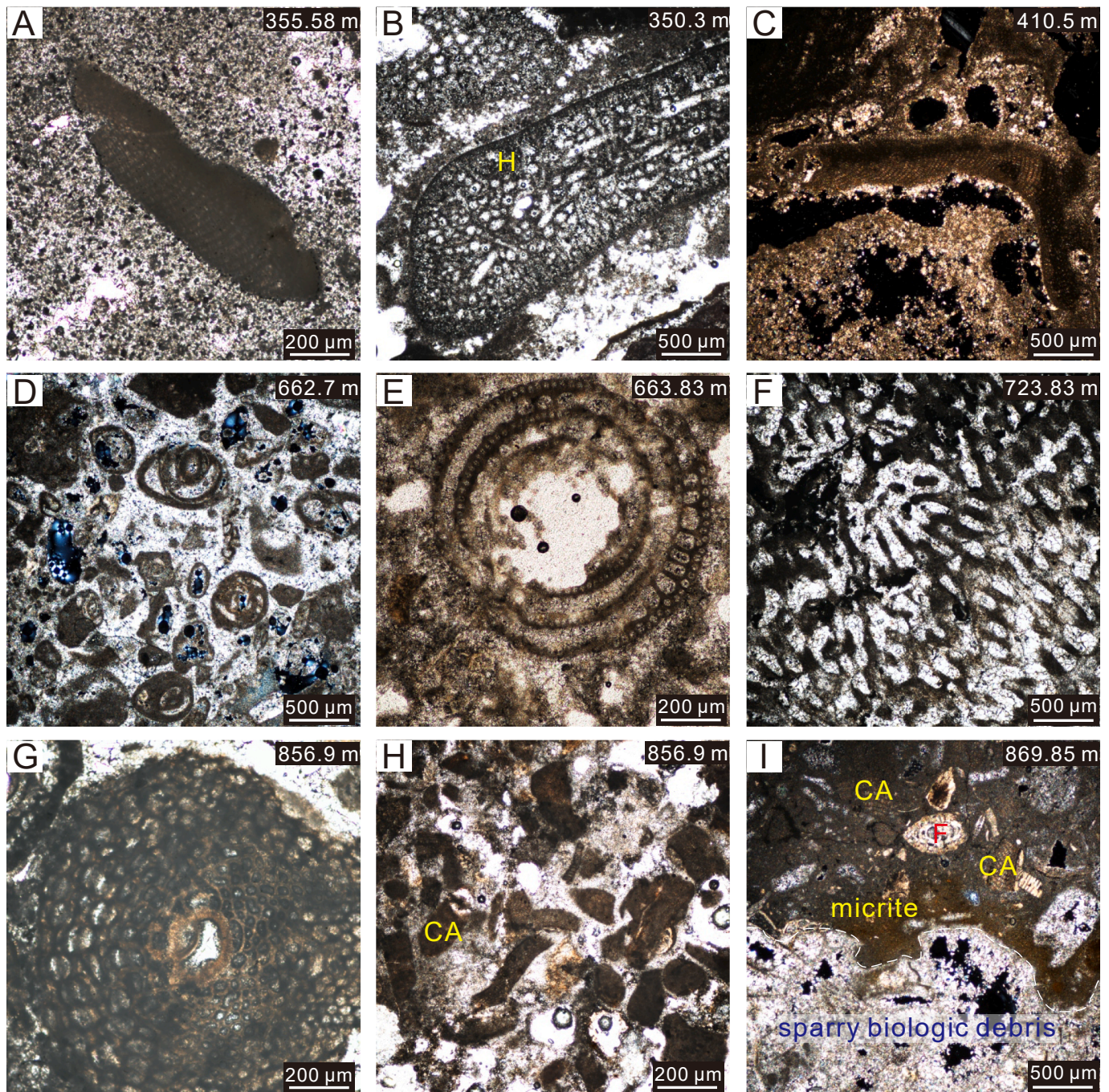
Fig. 5. Microfacies of the Miocene succession of Well CK2 including **A** crustose coralline algal branching floatstone (sample CK2-SY119), **B** well-preserved *Halimeda* (H) (sample CK2-SY118), **C** dolomitized sparry biologic debris (sample CK2-SY136), D well-preserved foraminifera (sample CK2-SY146), **E** chamber to dissolve large miliolids (sample CK2-SY147), **F** corals (sample CK2-SY152), **G** well-preserved bryozoan (sample CK2-SY163), **H** developed articulated coralline algae (CA) (sample CK2-SY163), and **I** the boundary between micrite and sparry calcite (white dotted line) (Sample CK2-SY166).

microfacies of this subunit, while LBF are a minor component.

The analyses of 12 thin sections in this area show that the coralline algal abundance ranges from 0 to 55.9%, averaging at 5.8%, while the coralline algal diversity is relatively low (Fig. 3). The assemblage includes non-geniculate and geniculate coralline algae. *Lithophyllum*, *Jania*, *corallina*, and *Hydrolithon* represent the most common coralline algal genera, which dominate the assemblage and characterize the CAA4 (Fig. 4).

Corals are abundant in this subunit (Fig. 3) and mainly include massive *Porites*, *Platygyra*, *Turbinaria*, *Hydnophora*, *Dipsastraea*, and branching *Acropora*.

3.2.4. Subunit i

Subunit *i* is approximately 8 m thick (506.1–489.44 m; 10–9.77 Ma) and primarily consists of coralline algal bindstones. Coralline algae and corals dominate the microfacies in this subunit.

The analyses of 9 thin sections of this subunit indicate a coralline algal abundance from 0 to 18%, averaging at 3%. The coralline algal diversity is moderate (Fig. 3) and the assemblage is dominated by non-geniculate forms. *Aethesolithon* and *Hydrolithon* represent the most common coralline algal genera (Fig. 6C). The genera *Aethesolithon* and *Hydrolithon* dominate the assemblage and characterize the CAA6 (Fig. 4).
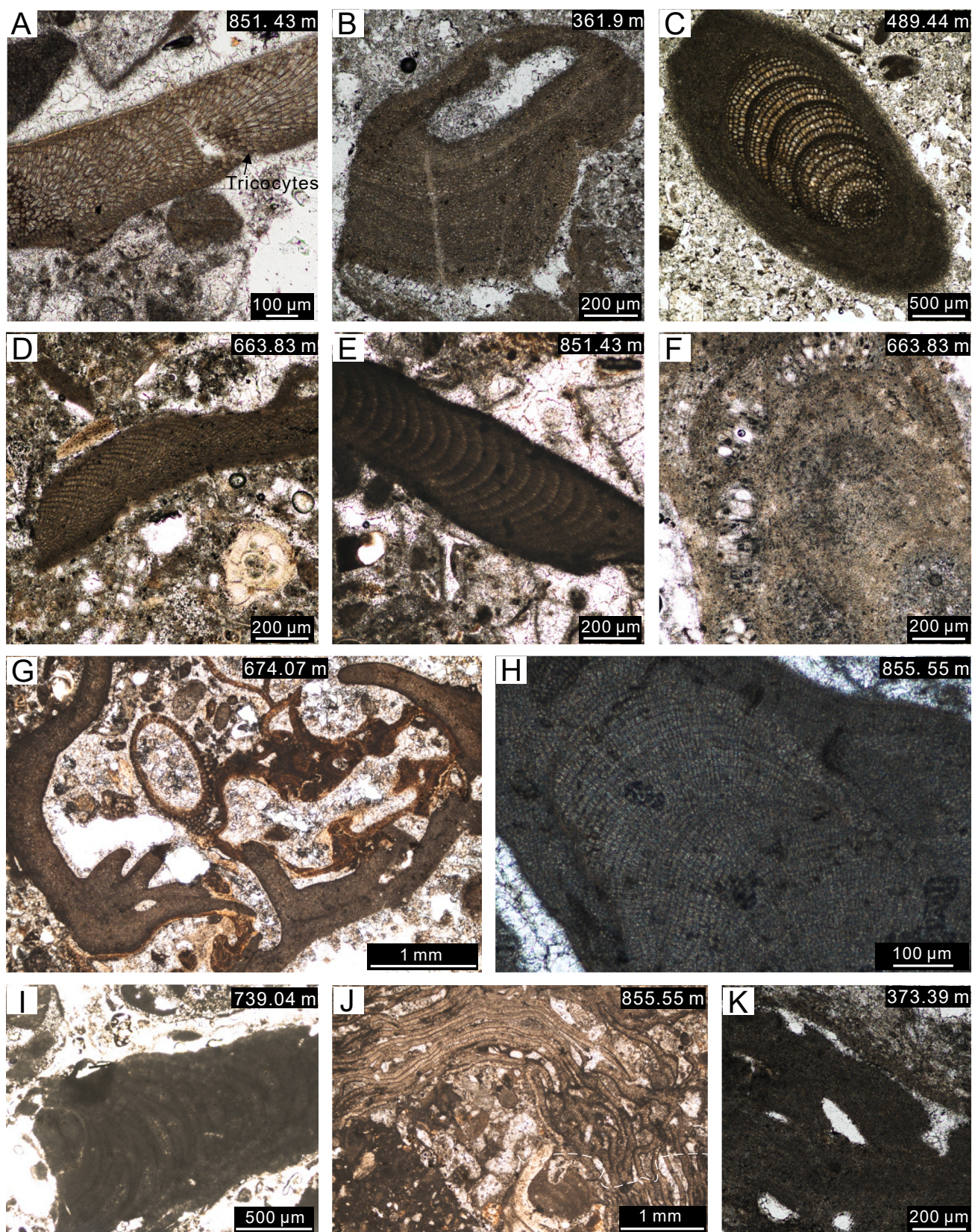
Fig. 6. Common coralline algae of Well CK2 including **A** *Neogoniolithon* sp. (sample CK2-SY162), **B** Corallinales (sample CK2-CB4), **C** *Aethesolithon nanhaiensis* (sample CK2-CZ4), **D** *Mesophyllum* sp. (sample CK2-SY147), **E** *Corallina* sp. (sample CK2-SY162), **F** *Sporolithon* sp. (sample CK2-SY147), **G** *Lithophyllum pseudoamphiroa* (sample CK2-S216), **H** *Lithophyllum* (sample CK2-S274), **I** *Lithothamnion* sp. (sample CK2-SY156), **J** *Lithoporella melobesioides* (sample CK2-S274), and **K** *Lithophyllum* sp. (sample CK2-CB5).
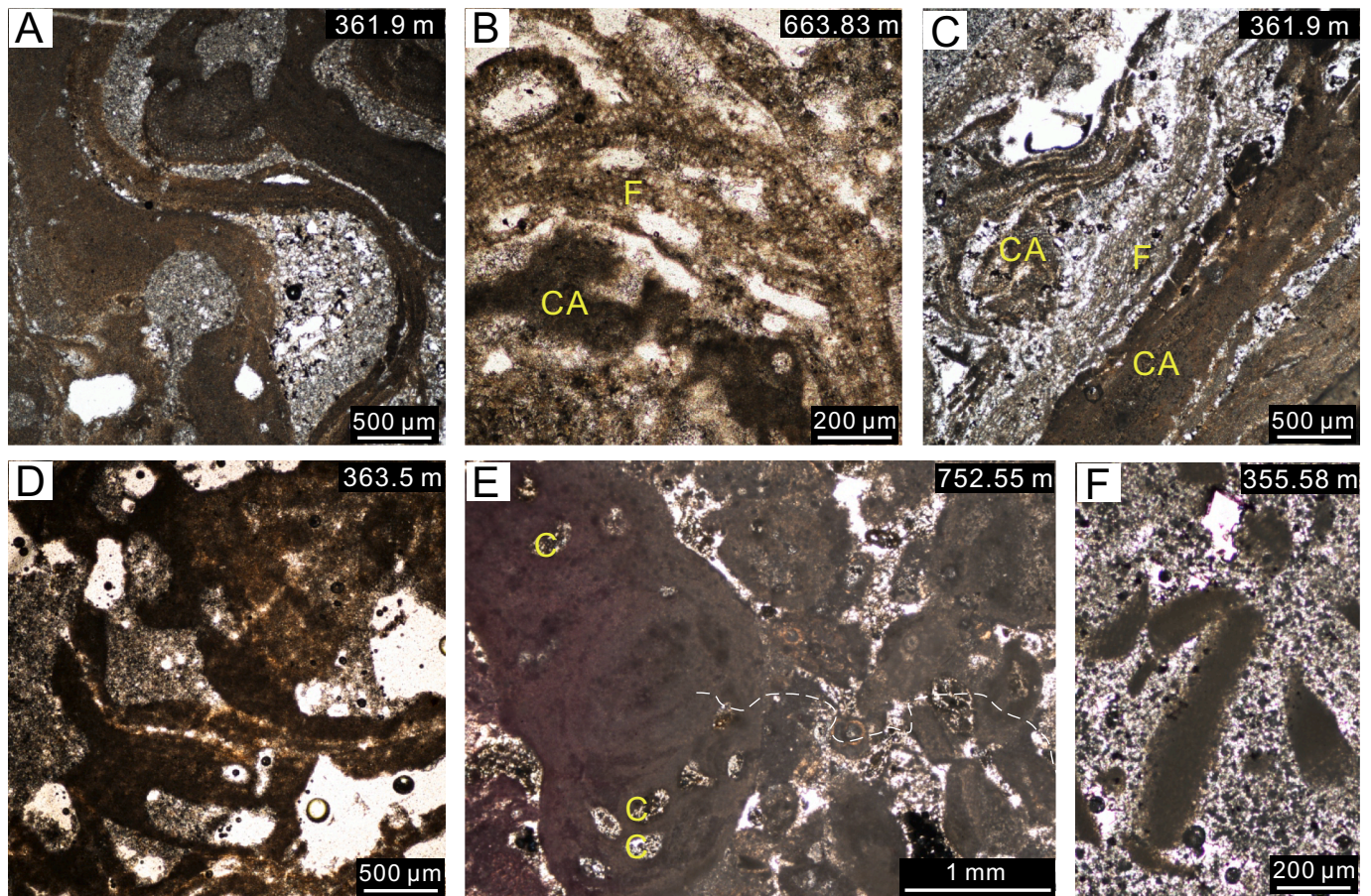
Fig. 7. Main lithological types of coralline algae in Well CK2 include **A** coralline algal framestones (sample CK2-CB4), **B** and **C** for-algaliths formed by coralline algae (CA) and encrusting foraminifera (F) (samples CK2-SY147 and CK2-CB4, respectively), **D** coralline algal bindstones (sample CK2-SY120), **E** coralline algal filling deposits (C: conceptacle) (sample CK2-S240), and **F** coralline algal floatstones (sample CK2-SY119).

Corals are abundant (Fig. 3) and include massive *Astreopora*, *Turbinaria*, and free-living *Fungia*.

3.2.5. Subunit j

Subunit *j* is 88 m thick (489.44–410 m; 9.77–7.35 Ma) and consists almost entirely of dolomitized wackestones, including sandy and micritic wackestones, as well as coralline algal wackestones. The skeletal assemblage mainly consists of corals and coralline algae (Fig. 5C).

The analyses of 31 thin sections in this area indicate a coralline algal abundance ranging from 0 to 45.4%, with an average of 9.1%, and a moderate diversity (Fig. 3). Coralline algae in this subunit are non-geniculate and geniculate, with *Mesophyllum* and *Lithophyllum* representing the most common coralline algal genera. In addition, we also identified rare specimens of *Lithothamnion*, *Corallina*, as well as other Hapalidiales and Corallinales. Overall, CAA5 dominates the assemblage (Fig. 4).

Coral abundance ranges from rare to abundant (Fig. 3). Specifically, at the base (489.44–474.61 m) and at the top (429.12–417.79 m) of this subunit, corals are rare and mainly represented by free-living *Fungia*. At 474.61–429.12 m, coral abundance is high, with massive *Turbinaria*, *Porites*, *Platygyra*, *Hydnophora*, *Favites*, and branching *Acropora*. Corals are present at 417.79–411.05 m (mainly free-living *Fungia*) and are absent at 411.05–410 m.

3.2.6. Subunit k

Subunit *k* is 88 m thick (410–344 m, 7.35–5.3 Ma) and mainly consists of coralline algal wackestones (Fig. 5A, 7F) and coralline algal bindstones (Fig. 7D) associated with coral framestones and coralline

algal framestones (Fig. 7A). The limestone is dolomitic and the skeletal assemblage includes corals and coralline algae; moreover, rare *Halimeda* was also observed (Fig. 5B).

The analyses of 37 thin sections in this area indicate a coralline algal abundance from 0 to 54.4%, with an average of approximately 9.3%, and a relatively high coralline algal diversity (Fig. 3). Algal types include non-geniculate and geniculate. For-algaliths occur in the upper part of this subunit (Fig. 7C). The most common coralline algal genera are represented by *Mesophyllum*, *Lithothamnion*, and *Lithophyllum* (Fig. 6K), while *Hydrolithon*, *Neogoniolithon*, *Jania*, other Corallinales (Fig. 6B), and species of an unidentified genus occurred as minor components. In this subunit, the genera *Mesophyllum*, *Lithothamnion*, and *Lithophyllum* dominate the assemblage and characterize the CAA7 (Fig. 4).

Coral abundance ranges from absent to abundant (Fig. 3), with corals developing alternately. Between 406.4 and 378.6 m and between 372 and 364.1 m, coral abundance is high and consists of massive *Turbinaria*, *Galaxea*, *Porites*, free-living *Fungia*, and foliated *Montipora*. However, corals do not occur in the remaining part of this subunit.

4. Discussion

4.1. Paleobathymetric significance of CAAs

As a biological indicator, coralline algae are widely used to reconstruct relative sea-level curves (Abbey et al., 2011; Coletti and Basso, 2020; Iryu et al., 2010). The reliability of reconstruction depends on the accuracy of identification and on the information available on a certain taxa or a certain assemblage (Abbey et al., 2011; Braga and Aguirre,

2004).

4.1.1. Corallina-Jania-Hydrolithon-Lithoporella assemblage (CAA1)

As a significant biotic component of rocky shores and rock pools in the North Atlantic (Williamson et al., 2015), *Corallina officinalis* (Linnaeus 1758) occurs in the intertidal rock pools at depths of ±0.3 m during low tide in St. Margaret's Bay, United Kingdom (Rendina et al., 2019). *Jania rubens* grow abundantly in shallow water (Bueno et al., 2016) in the form of epiphytic or epilithic turfs (Porzio et al., 2018). *Hydrolithon onkodes* with branching *Acropora* also grow in shallow-waters (Abbey et al., 2011). In Well CK2, the interval during the occurrence of this assemblage is associated with the presence of branching *Acropora* corals. Therefore, a water depth of less than 5 m is proposed for CAA1.

4.1.2. Mesophyllum assemblage (CAA2)

Mesophyllum usually distributes into deep-water and intermediate depth communities, often in CAAs of Ryukyu Islands in reef slope at depths of 15 to 30 m (Iryu, 1992; Iryu et al., 1995). This assemblage indicates a relatively deep-water environment, as previously discussed by Li et al. (2021). During the development of this assemblage, corals were absent, and other coralline algae remained undeveloped. According to the Quaternary water depth environment of Well CK2, *Mesophyllum* assemblages developed in a lagoon sedimentary environment of 15 to 25 m of water depth.

4.1.3. Hydrolithon-Lithoporella-Lithophyllum assemblage (CAA3)

Li et al. (2021) argued that the *Lithoporella-Lithophyllum* assemblage of Well CK2 is indicative of shallow-water within a 15 m depth, and thus developed in an outer reef flat setting. *Hydrolithon onkodes* may occur in this type of shallow-water environments, particularly in high-energy settings (around 5 m of water depth; Cabioch et al., 1999a). The association of massive corals such as *Porites* and encrusting algae *Mesophyllum*, requiring relatively deep waters or shaded rocky environments, with CAA3, suggest that this assemblage might have developed slightly deeper than CAA1, at approximately 10 m of water depth.

4.1.4. Corallina-Jania-Hydrolithon-Lithophyllum assemblage (CAA4)

In modern coral reefs, *Corallina*, *Jania*, and *Hydrolithon* mainly occur in shallow-water environments. *Lithophyllum* usually distributes in a water depth of approximately 20 m (Bosence, 1991). It also grows on the rocks within 10 to 12 m water depths, and make up algal nodules (Adey, 1986; Braga and Aguirre, 2004), and can build large "trottoirs" in the intertidal zone in the Mediterranean (Adey, 1986; Braga and Aguirre, 2001). *Lithophyllum tessellatum* Lemoine (as *Dermatolithon tessellatum*) mainly distributes into water depths within 10 m (Cabioch et al., 1999b). In addition, *Amphistegina* and *Heterostegina*, indicative of shallow-water conditions, are also abundant in this assemblage. Compared with CAA1, *Mesophyllum* and *Lithothamnion* representing deep-water environments occur in the interval of distribution in CAA4, which may have grown under shaded rocks in the past. Overall, CAA4 is related to a reef flat sedimentary environment within a depth of 10 m.

4.1.5. Mesophyllum-Lithophyllum assemblage (CAA5)

In the Southwest Atlantic Ocean, *Mesophyllum macroblastum* occurs in the depths within 15 m (Bahia et al., 2014). In the northwestern Mediterranean, the coralligenous, community dominated by *Mesophyllum alternans* and *Lithophyllum frondosum*, occurs in the depths ranging from 15 to 30 m (Garrabou and Ballesteros, 2000). Furthermore, *Mesophyllum* commonly occurs in the depths ranging from 15 to 30 m in the Ryukyu Group (Iryu, 1992; Iryu et al., 1995). In addition, the paleobathymetric changes recorded by coralline algae in Well CK2 since the Pliocene show that the *Mesophyllum-Lithophyllum* assemblage represents the sedimentary environment of a 15–20 m lagoon slope (Li et al., 2021). In the present study, the biota diversity increased from 16.78 Ma to 16.31 Ma. During this period, *Acropora* coral developed, unlike *Hydrolithon.* These findings suggest that the presence of the *Mesophyllum-Lithophyllum* assemblage indicates a relatively deep-water environment or lagoon patch reef/lagoon slope sedimentary environment.

4.1.6. Hydrolithon-Aethesolithon assemblage (CAA6)

Although the distribution of *Aethesolithon* is evident since early Miocene to the present, relatively few fossil reports are available on this genus. *Aethesolithon* is abundant in shallow-water reef settings in the Pacific Ocean (Peña et al., 2018), Pleistocene shallow-water reef deposits in the northeast of Australia (Braga and Aguirre, 2004), and middle Miocene reefs of East Kalimantan (Rösler et al., 2015). In the Maldives, *Aethesolithon* dominates the shallow-water reefal assemblages in the middle Miocene (Reolid et al., 2020). Since *Hydrolithon* is a shallow water dweller that often develops algal ridges (Adey, 1986), the CAA6 assemblage could be related to a shallow (< 5 m of water depth) reef flat environment.

4.1.7. Mesophyllum-Lithothamnion-Lithophyllum assemblage (CAA7)

In modern coral reefs, the abundance of *Mesophyllum* and *Lithothamnion* increases with increasing water depth (Adey, 1986; Iryu et al., 2010). They generally appear below 20 m and can occur up to depths of 110–120 m (Adey, 1986; Braga and Aguirre, 2004; Lund et al., 2000; Sarkar, 2017). In the Great Barrier Reef, CAAs dominated by *Mesophyllum* and *Lithothamnion* represent the biozone below 10–15 m depths (Braga and Aguirre, 2004). Similarly, in the Sulawesi Archipelago, Indonesia, this assemblage is found at a depth below 15 m (Braga and Aguirre, 2004). In the Indo-Pacific, *Lithothamnion prolifer* occurs at depths of 20–40 m (Keats et al., 1996). In Fraser Island, Queensland, *Mesophyllum*, *Lithothamnion*, and *Sporolithon* are characteristic of outer platform settings (below 35–50 m) and are also distributed in dark or shaded locations (caves and fissures) (Abbey et al., 2011; Lund et al., 2000). In Well CK2, the development of this assemblage is accompanied by the distribution of *Turbinaria* and *Porites* corals. Coral assemblages dominated by *Turbinaria* occurred in the middle to lower reef slopes (Humblet et al., 2009), whereas assemblages of *Porites* can occur in a maximum water depths of 30 m (Cabioch et al., 1999a). Consistently, this assemblage is attributed to water-depth of more than 20 m.

4.2. Comparison of sea-level changes reconstructed using CAAs with global sea level changes

Data on Cenozoic global sea-level curves have been evaluated and updated over the last four decades (Braithwaite, 2016; Haq et al., 1987; Miller et al., 2005; Miller et al., 2020). During the Miocene, global sea levels showed a long-term regressive trend, particularly at 15–10 Ma, followed by a gradual increase (Haq et al., 1987). A series of major climatic and environmental events occurred during this period, such as significant temperature and precipitation changes in the MCO (~17–14.5 Ma), increased biodiversity (Kohn and Fremd, 2008), and significant changes in biological habitats (Retallack, 2007). Furthermore, the middle Miocene, the key period of the Earth's climate, is characterized by the gradual change from warm to cooler environments due to major environmental changes (Baldassini et al., 2021). At a range of 17 to 14.55 Ma, the warm surface water, oligotrophic, high salinity and restricted environment is followed by an open marine environment remaining under warm surface water and oligotrophic conditions (Baldassini et al., 2021). Following the relatively MCO from ~17 to 15 Ma in the middle Miocene, atmospheric cooling may lead to and trigger the largest ice-sheet (Lewis et al., 2007). The middle Miocene climate transition (~14.1–13.8 Ma) is an important ice growth event (Zachos et al., 2001), related to the growth and the stabilization of the Antarctic ice sheet (Catherine, 2020). The amplitude of Antarctic ice growth and rapid climate transition show that the Earth's climate system is sensitive to the ocean and cryospheric feedbacks as well as the atmosphere (Shevenell et al., 2004).

Based on the relationship between CAAs and their present water depth distribution, we reconstructed the Miocene sea-level changes in the SCS. Our results show that the seven observed CAAs suggest that the water-depth fluctuated between 5 and more than 25 m (Fig. 8). The base of the first sedimentary cycle (19.6–16.31 Ma) is characterized by CAA1, which is then replaced by CAA2, indicating a deep-water environment, and thus, a rise in the relative sea level. During this period, the global sea level rose from the lowest −50 m to +30 m (Miller et al., 2020). The overlying CAA3 and CAA4 instead testify more shallow condition indicting a continuous decline in sea level. Furthermore, The global sea-level oscillation was relatively small during this period (Miller et al., 2020). The CAA5 assemblage on the other hand testify to a new period of transgression (Fig. 8). The global sea level was in a stage of rapid rise during 16.93–16.31 Ma, with the maximum rise of approximately +50 m (Miller et al., 2020). Thus, the sea-level changes in the first sedimentary cycle exhibit a rise-fall-rise pattern. In the second sedimentary cycle (16.31–5.3 Ma), six CAAs were recorded with the sea level change pattern similar to those of the first sedimentary cycle. CAA1 dominates the assemblage of the base of the second sedimentary cycle, and replaced by CAA2 and CAA4. CAA6 only developed between 10 and 9.77 Ma, thereby indicating a relatively very shallow reef crest/flat sedimentary environment, thus representing a sea level minimum during this period. Subsequently, the CAAs were successively replaced by CAA5 and CAA7, indicating a continuous increase in the sea level. From 16.31 to 9.77 Ma, the global sea level also showed a downward trend (Fig. 8; Miller et al., 2020).

A comparison of the reconstructed relative sea levels in this study with global sea-level changes showed similar long-term shifts, thereby validating the accuracy of the proposed method. In addition, the results of the reconstructed sea-level changes are consistent with changes in oxygen isotopes of foraminifera in the SCS (Wang et al., 2003).

4.3. Validating the reliability of reconstructed sea levels

The "Keep-up", "Catch-up", and "Give-Up" stages of coral reefs are controlled by tectonics, sea level changes, as well as paleoceanic and climatic conditions (Schlager, 1981; Schlager, 1999; Jiang et al., 2019; Wu et al., 2019). Therefore, in the present study, based on the "Keep-up", "Catch-up", and "Give-Up" (drowning) stages of coral reefs, the sea-level changes in the Miocene were reconstructed to prove the reliability of the sea-level curves reconstructed by CAAs.

4.3.1. Miocene reef "keep-up" stage

During the early Miocene, the extension of the ice caps was still limited during this period, leading to small 30/40 m sea-level oscillations (Miller et al., 2020). The Xisha uplift gradually subsided with the post-rift thermal reduction of the lithosphere in the northernregions of the SCS, leading to marine transgression over the subsiding volcanic basement of the Xisha Islands during this period (Wu et al., 2019). However, the weak East Asian monsoon in the early Miocene prevented the upwelling from reaching the Xisha Islands, leading to relatively warm and oligotrophic water over the area (Wu et al., 2019). In this
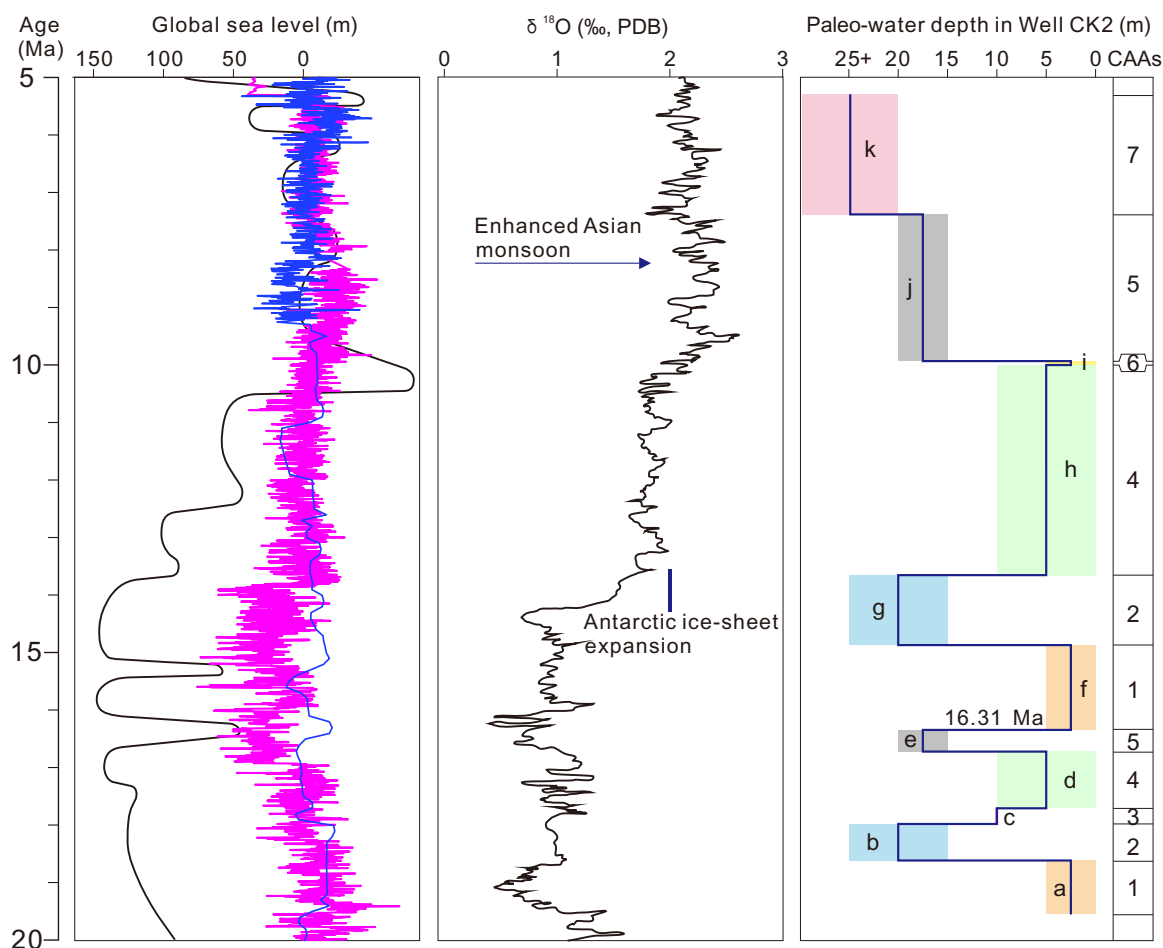
Fig. 8. Global sea level and paleowater depth curves related to Well CK2. Global sea-level curves (black, blue, and pink) were obtained from Haq et al. (1987), Miller et al. (2005), and Miller et al. (2020), respectively. Oxygen isotope curves were obtained from Wang et al. (2003). The paleo-water depth curves in this study were reconstructed based on the different subunits (*a*, *b*, …, *k*) dominated by coralline algal assemblages (CAAs). Arabic numerals represent different CAAs. (For interpretation of the references to color in this figure legend, the reader is referred to the web version of this article.)

setting, a suitable basement and water depth are the primary limiting factors for reef development. Consistently, the first colonizer of the volcanic basement are represent by very shallow. In Well CK2, the bottom of approximately 50 m consists of volcanic rocks (Fan et al., 2020). The coral reef initially developed over this volcanic bedrock at 19.6 Ma (Fan et al., 2020). The assemblage (CAA1) directly overlying the basement consists of shallow-water corals (massive *Asteropora*) and coralline algae (e.g. *Corallina* and *Jania*), supporting a relatively shallow conditions during transgression initiation. At an early stage of coral reef development, coralline algae are primarily branching, and the sedimentation rate is relatively high (Fig. 2; Fan et al., 2020), suggesting that the reef forming rate is faster during the early stages of coral reef development. However, the sea level rising rate constrained the development of coral reefs at 19.6–18.67 Ma (subunit *a*), when coral reefs showed a "keep-up" model.

4.3.2. Miocene reef "catch-up" stage

The alternate development of shallow-water CAAs in subunit (*c*, *d*, and *f*) and relatively deep water CAAs in subunit *e* at the bottom of Well CK2 indicates continuous fluctuation in biological assemblages within their maximum tolerated microenvironment. Within this range, the coral morphology exhibits a similar pattern, alternating between the three forms of massive, branching, and encrusting. Reef-building organisms migrate to shallow uplands to allow for growth within suitable water depths. The evidence suggests that, during their development, coral reefs follow relative sea-level fluctuations and were in a "catch-up" stage. Furthermore, at 16–15 Ma, planktonic foraminifera was in abundance, accompanied by coralline algal bindstones and coral gravel, such as *Porites* coral. The sediments in this facies zone were mainly composed of lagoon sand. *Porites* coral develops in the sheltered reef flats, patch reefs, or reef backs at depths of 0–25 m (Cabioch et al., 1999b). Therefore, it can be inferred that the coral reefs of Well CK2 developed as small patch reefs within a lagoon at 16–15 Ma, with a continuous expansion in the reef range. Thereafter, the vertical deposition of coral reefs occurred at an extremely slow pace, indicating a fall in the relative sea level, and the possible progradation of the coral reef. At 13–11 Ma, the biodiversity of the coral reef ecosystem markedly decreased, as indicated by the sporadic distribution of branching Corallinales, and reef development was reduced. At 11 Ma, coralline algae and corals were absent, and the sedimentation rate was relatively low (4.5 m/Myr; Fan et al., 2020). At 10–9.77 Ma, the reefs regained their self-development with CAA6, in the shallowest water settings. During these periods, CAAs (CAA4 and CAA6; subunit *h* and subunit *i*) in shallow water environment dominated the assemblage. Furthermore, the unconformity at 10.16 Ma (519 m; Wang et al., 2018) indicates that the development of coral reefs in this period was controlled by the continuous decline of sea level. These findings characterize a shallow upward environment, indicating coral reef in a "catch-up" stage. After 9.47 Ma, global geological events occurred frequently along with severe climatic changes (Zachos et al., 2001); thus, the coral reefs in the SCS re-entered a fluctuation stage. In subunit *j* (9.77–7.35 Ma), the pioneer groups in shallow water were replaced by deep-water assemblages as the sea level rose, and the development of coral reefs has entered the "catch-up" stage. The global sea level corresponding to these periods showed a gradual downward trend (Miller et al., 2020). In addition, the tectonic subsidence rate of Xisha Islands was also low during these period (Wu et al., 2018), which is also agreement with the "catch-up" developmental model of coral reefs.

4.3.3. Miocene reef "give-up" stage

The reefs experienced a rapid development between 19.6 and 18.67 Ma (subunit *a*: 873.55–838.05 m), along with a rapid increase in the relative sea levels during this period. At 18.67–17.98 Ma (subunit *b*: 838.05–801.15 m), corals were absent/rare, whereas CAA2 developed in this interval but with reduction marked decrease in the sedimentation rate (Fig. 2; Fan et al., 2020). The relative sea level presumably

increased, with the coral reefs in or near the drowning (give-up) stage. Similar to subunit *b*, subunit *g* (14.79–13.72 Ma) is also dominated by CAA2 indicating a deep-water environment, suggesting that coral reefs are also in a "give-up" stage during this period. At 7.35–5.3 Ma (subunit *k*), CAA7 in deep water environment dominate the assemblage. The sedimentation rate was relatively low (Fan et al., 2020). Furthermore, with the deepening trend of paleo-water depth, coral abundance becomes rare/absent. These findings suggest that the continuous rise of sea level during these periods constraint the development of coral reefs, resulting in "give-up" stages. The global sea level also rose during these periods. In addition, the subsidence of Xisha Islands accelerated at 10.5–5.5 Ma (Wu et al., 2018), which also proved that the coral reefs were in a "give-up" stage at 7.35–5.3 Ma.

Taken together, the Miocene relative sea-level changes recorded by the development of coral reefs in the Xisha Islands are consistent with long-term global sea-level changes and validate the reliability of using sea-level history as recorded by CAAs.

5. Conclusions

In our study, 11 genera of coralline algae were identified in Well CK2, consisting of seven coralline algal assemblages. The occurrence of *Corallina-Jania-Lithoporella-Hydrolithon* assemblage between 19.6 and 18.67 Ma and between 16.31 and 14.79 Ma is indicative of shallow-water environments with depths of 5 m during this period. *Mesophyllum* assemblage at 18.67–17.98 Ma and 14.79–13.72 Ma, represents water depths of 15–25 m. The presence of *Lithoporella-Hydrolithon-Lithophyllum* assemblage from 17.98 Ma to 17.73 Ma indicates approximate water depths of ~10 m. At 17.73–16.31 Ma, the *Corallina-Jania-Hydrolithon-Lithophyllum* assemblage is replaced by the *Mesophyllum-Lithophyllum* assemblage, indicating a deepening of water depths. At 13.72–10 Ma, branching CAA sporadically developed, indicating a water-depth of approximately 10 m. The *Hydrolithon-Aethesolith* assemblage dominates at 10–9.77 Ma and is representative of very shallow (5 m or less), high energy conditions. *Mesophyllum-Lithophyllum* assemblage represents relatively shallow settings (15–20 m). At 7.35–5.3 Ma, the reef settings were relatively deep (> 20 m), as represented by *Mesophyllum-Lithothamnion-Lithophyllum* assemblage and *Turbinaria*, *Porites*, and *Fungia*. Along with the rising sea levels, the coral reefs also developed rapidly in the early Miocene. Pioneer reef-building organisms are mainly branching coralline algae and massive corals, found during the initial stages of coral reef development. At 16.78–16.31 Ma, the coralline algal diversity significantly increased. The massive *Porites* coral and coralline algal bindstones developed from 16 Ma to 15 Ma, indicating a small lagoon depositional environment related to the patch reef. At 8.7–7.35 Ma, the coralline algal diversity suddenly increased with a gradual increase in sea levels, suggesting a short-term prosperous coral reef stage. At 7.35–5.3 Ma, the increased biodiversity and developed free-growing *Fungia* without *Acropora* are indicatives of the deep water, shade, and relatively low visibility reef environment. Furthermore, six developmental stages of the Miocene coral reef were recognized based on relationship between coral reef development and changes in water depth, including a "keep-up" stage (19.6–18.67 Ma), three "give-up" stages (18.67–17.98 Ma; 14.79–13.72 Ma; and 7.35–5.3 Ma), and two "catch-up" stage (17.98–16.31 Ma; 13.72–7.35 Ma). Our findings suggest that it is feasible to restore the sea-level history with coralline algae from coral reefs; however, the study of multiple drilling cores will increase the applicability of our findings, and allow us to better investigate the relationship between the evolution of coralline algal assemblages and the environment.

Declaration of Competing Interest

This manuscript has not been published or presented elsewhere, in part or in entirety, and is not under consideration by another journal. We have read and understood your journal's policies, and we believe that

neither the manuscript nor the study violates any of these. There are no conflicts of interest to declare.

Acknowledgments

Appendix A. Supplementary data

Supplementary data to this article can be found online at https://doi.org/10.1016/j.palaeo.2021.110673.

References

Abbey, E., Webster, J.M., Braga, J.C., Sugihara, K., Wallace, C., Iryu, Y., Potts, D., Done, T., Camoin, G., Seard, C., 2011. Variation in deglacial coralgal assemblages and their paleoenvironmental significance: IODP Expedition 310, "Tahiti Sea Level". Glob. Planet. Chang. 76 (1), 1–15.

Adey, W.H., 1986. Coralline algae as indicators of sea-level. In: van de Plassche, O. (Ed.), Sea-Level Research: A Manual for the Collection and Evaluation of Data. Geo-Books, Norwich, pp. 229–280. https://doi.org/10.1007/978-94-009-4215-8_9.

Adey, W.H., Macintyre, I.G., 1973. Crustose coralline algae: a re-evaluation in the geological sciences. Geol. Soc. Am. Bull. 84 (3), 883–904.

Aguirre, J., Riding, R., Braga, J.C., 2000. Diversity of coralline red algae: origination and extinction patterns from the early cretaceous to the Pleistocene. Paleobiology 26 (4), 651–667.

Bahia, R.D., Amado, G.M., Azevedo, J., Maneveldt, G.W., 2014. Porolithon improcerum (Porolithoideae, Corallinaceae) and Mesophyllum macroblastum (Melobesioideae, Hapalidiaceae): new records of crustose coralline red algae for the Southwest Atlantic Ocean. Phytotaxa 190 (1), 38–44.

Baldassini, N., Foresi, L.M., Lirer, F., Sprovieri, M., Turco, E., Pelosi, N., Stefano, A.D., 2021. Middle Miocene stepwise climate evolution in the Mediterranean region through high-resolution stable isotopes and calcareous plankton records. Mar. Micropaleontol. 167, 102030.

Bard, E., Hamelin, B., Arnold, M., Montaggioni, L., Rougerie, F., 1996. Deglacial Sea-level record from Tahiti corals and the timing of global meltwater discharge. Nature 382 (6588), 241–244.

Bassi, D., Braga, J.C., Iryu, Y., 2009. Palaeobiogeographic patterns of a persistent monophyletic lineage: Lithophyllum pustulatum species group (Corallinaceae, Corallinales, Rhodophyta). Palaeogeogr. Palaeoclimatol. Palaeoecol. 284 (3), 237–245.

Bosence, D.W., 1983. Description and Classification of Rhodoliths (Rhodoids, Rhodolites). In Coated grains. Springer, Berlin, Heidelberg, pp. 217–224.

Bosence, D.W.J., 1991. Coralline algae: mineralization, taxonomy, and palaeoecology. Calcareous algae and Stromatolites 98–113.

Bradshaw, C.D., 2021. Miocene Climates. IN: Encyclopedia of Geology (Second Edition), pp. 486–496.

Braga, J.C., Aguirre, J., 1995. Taxonomy of fossil coralline algal species: Neogene Lithophylloideae (Rhodophyta, Corallinaceae) from southern Spain. Rev. Palaeobot. Palynol. 86 (3–4), 265–285.

Braga, J.C., Aguirre, J., 2001. Coralline algal assemblages in upper Neogene reef and temperate carbonates in Southern Spain. Palaeogeography Palaeoclimatology Palaeoecology 175 (1-4), 27–41. https://doi.org/10.1016/s0031-0182(01)00384-4.

Braga, J.C., Aguirre, J., 2004. Coralline algae indicate Pleistocene evolution from deep, open platform to outer barrier reef environments in the northern Great Barrier Reef margin. Coral Reefs 23 (4), 547–558.

Braga, J.C., Bassi, D., 2012. Neogene history of Sporolithon Heydrich (Corallinales, Rhodophyta) in the Mediterranean region. Palaeogeogr. Palaeoclimatol. Palaeoecol. 243 (1), 189–203.

Braga, J.C., Martín, J.M., 1996. Geometries of reef advance in response to relative sea-level changes in a Messinian (uppermost Miocene) fringing reef (Cariatiz reef, Sorbas Basin, SE Spain). Sediment. Geol. 107 (1–2), 61–81.

Braga, J.C., Bosence, D.W.J., Steneck, R.S., 1993. New anatomical characters in fossil coralline algae and their taxonomy implications. Palaeontology 36 (3), 535–547.

Braithwaite, C.J.R., 2016. Coral-reef records of Quaternary changes in climate and sea-level. Earth-Sci. Rev. 156, 137–154.

Bueno, M., Dena-Silva, S.A., Flores, A.A.V., Leite, F.P.P., 2016. Effects of wave exposure on the abundance and composition of amphipod and tanaidacean assemblages inhabiting intertidal coralline algae. Journal of the Marine Biological Association of the United Kingdom 96 (3), 761–767. https://doi.org/10.1017/s002531541500123x.

Cabioch, G., Camoin, G., Montaggioni, L.F., 1999a. Postglacial growth history of a French Polynesian barrier reef tract, Tahiti, Central Pacific. Sedimentology 46 (6), 985–1000.

Cabioch, G., Montaggioni, L.F., Faure, G., Ribaud-Laurenti, A., 1999b. Reef coralgal assemblages as recorders of paleobathymetry and sea level changes in the Indo-Pacific province. Quat. Sci. Rev. 18 (14), 1681–1695.

Camoin, G.F., Colonna, M., Montaggioni, L.F., Casanova, J., Faure, G., Thomassin, B.A., 1997. Holocene Sea level changes and reef development in the southwestern Indian Ocean. Coral Reefs 16 (4), 247–259.

Camoin, G.F., Montaggioni, L.F., Braithwaite, C.J.R., 2004. Late glacial to post glacial sea levels in the Western Indian Ocean. Mar. Geol. 206 (1), 119–146.

Catherine, D.B., 2020. Miocene Climates (Reference Module in Earth Systems and Environmental Sciences).

Coletti, G., Basso, D., 2020. Coralline algae as depth indicators in the Miocene carbonates of the Eratosthenes Seamount (ODP Leg 160, Hole 966F). Geobios 60, 29–46.

Coletti, G., Basso, D., Corselli, C., 2018. Coralline algae as depth indicators in the Sommières Basin (early Miocene, Southern France). Geobios 51, 15–30.

Coletti, G., Basso, D., Betzler, C., Robertson, A.H.F., Spezzaferri, S., 2019. Environmental evolution and geological significance of the Miocene carbonates of the Eratosthenes Seamount (ODP Leg 160). Palaeogeogr. Palaeoclimatol. Palaeoecol. 530, 217–235.

Embry, A.F., Klovan, J.E., 1971. A late Devonian reef tract on northeastern Banks Island, N.W.T. Bull. Can. Petrol. Geol. 19, 730–781.

Fan, T., Yu, K., Zhao, J., Jang, W., Xu, S., Zhang, Y., Wang, R., Wang, Y., Feng, Y., Bian, L., Qian, H., Liao, W., 2020. Strontium isotope stratigraphy and paleomagnetic age constraints on the evolution history of coral reef islands, northern South China Sea. Geological Society of America 131, 1–14.

Garrabou, J., Ballesteros, E., 2000. Growth of Mesophyllum alternans and Lithophyllum frondosum (Corallinales, Rhodophyta) in the northwestern Mediterranean. British Phycological Bulletin 35 (1), 1–10.

Ginsburg, R.N., Schroeder, J.H., 2010. Growth and Submarine Fossilization of Algal Cup Reefs, Bermuda. Sedimentology 20 (4), 575–614.

Halfar, J., Mutti, M., 2005. Global dominance of coralline red-algal facies: a response to Miocene oceanographic events. Geology 33, 481–484.

Hallmann, N., Camoin, G., Eisenhauer, A., Vella, C., 2013. Reconstruction of Late Holocene Sea-Level Change in French Polynesia, South Pacific, Based on Coral Reef Records (Egu General Assembly Conference).

Haq, B.U., Hardenbol, J., Vail, P.R., 1987. Chronology of fluctuating sea levels since the triassic. Science 235 (4793), 1156–1167.

Harvey, A.S., Broadwater, S.T., Woelkerling, W.J., Mitrovski, P.J., 2003. Choreonema (Corallinales, Rhodophyta): 18S rDNA phylogeny and resurrection of the Hapalidiaceae for the subfamilies Choreonematoideae, Austrolithoideae, and Melobesioideae. J. Phycol. 39 (5), 988–998.

Hay, W.W., 2011. Can humans force a return to a 'cretaceous' climate? Sediment. Geol. 235 (1–2), 5–26.

Herbert, T.D., Lawrence, K.T., Tzanova, A., Peterson, L.C., Caballero-Gill, R., Kelly, C.S., 2016. Late Miocene global cooling and the rise of modern ecosystems. Nat. Geosci. 9, 843–847.

Humblet, M., Iryu, Y., Nakamori, T., 2009. Variations in Pleistocene coral assemblages in space and time in southern and northern Central Ryukyu Islands, Japan. Mar. Geol. 259, 1–20.

Humblet, M., Hongo, C., Sugihara, K., 2015. An identification guide to some major Quaternary fossil reef-building coral genera (Acropora, Isopora, Montipora, and Porites). Island Arc 24 (1), 16–30.

Iryu, Y., 1992. Fossil non-articulated coralline algae as depth indicators for the Ryukyu Group. Transactions and Proceedings of the Palaeontological Society of Japan 167, 1165–1179.

Iryu, Y., Nakamori, T., Matsuda, S., Abe, O., 1995. Distribution of marine organisms and its geological significance in the modern reef complexes of the Ryukyu Islands. Sediment. Geol. 99, 243–258.

Iryu, Y., Takahashi, Y., Fujita, K., Camoin, G., 2010. Sealevel history recorded in the Pleistocene carbonate sequence in IODP Hole 310-M0005D, off Tahiti. Island Arc 19 (4), 690–706.

Jian, L., Zhizheng, Y., Chunrui, H., Xinbo, L., Gaosheng, Q., 1997. Meteoric diagenesis in Pleistocene reef limestones of Xisha Islands, China. J. Asian Earth Sci. 15 (6), 465–476.

Jiang, W., Yu, K., Fan, T., Xu, S., Wang, R., Zhang, Y., Yue, Y., Zhao, J., Feng, Y., Wei, C., Wang, S., 2019. Coral reef carbonate record of the Pliocene-Pleistocene climate transition from an atoll in the South China Sea. Mar. Geol. 411, 88–97.

Keats, D.W., Steneck, R.S., Townsend, R.A., Borowitzka, M.A., 1996. Lithothamnion proliferum Foslie: a common non-geniculate coralline alga (Rhodophyta: Corallinaceae) from tropical and subtropical Indo-Pacific. Bot. Mar. 39, 187–200.

Kershaw, S., Guo, L., Braga, J.C., 2005. A Holocene coral-algal reef at Mavra Litharia, Gulf of Corinth, Greece: structure, history, and applications in relative sea-level change. Mar. Geol. 215 (3), 171–192.

Kohn, M.J., Fremd, T.J., 2008. Miocene tectonics and climate forcing of biodiversity, Western United States. Geology 36 (10), 783–786.

Le Gall, L., Payyri, C., Bittner, L., Saunders, G.W., 2009. Multigene phylogenetic analyses support recognition of the Sporolithales Ord. Nov. Mol. Phylogenet. Evol. 54, 302–305.

Lewis, A.R., Marchant, D.R., Ashworth, A.C., Hemming, S.R., Machlus, M.L., 2007. Major middle Miocene global climate change: evidence from East Antarctica and the Transantarctic Mountains. Geol. Soc. Am. Bull. 119, 1449–1461.

Li, Y., Yu, K., Bian, L., Fan, T., Wang, R., Jiang, W., Xu, S., Zhang, Y., Yang, Y., 2021. Paleo-water depth variations since the Pliocene as recorded by coralline algae in the South China Sea. Palaeogeogr. Palaeoclimatol. Palaeoecol. 562, 110107.

Lund, M., Davies, P.J., Braga, J.C., 2000. Coralline algal nodules off Fraser Island, eastern Australia. Facies 42, 25–34.

Ma, Y., Wu, S., Lv, F., Dong, D., Gu, M., 2011. Seismic characteristics and development of the Xisha carbonate platforms, northern margin of the South China Sea. Journal of Asian Earth ences 40 (3), 770–783.

Macintyre, I.G., Neumann, A.C., 2011. Reef Classification, Response to Sea Level rise. In: Hopley, D. (Ed.), Encyclopedia of Modern Coral Reefs. Encyclopedia of Earth Sciences Series. Springer, Dordrecht. https://doi.org/10.1007/978-90-481-2639-2_90.

Miller, K.G., Kominz, M.A., Browning, J.V., Wright, J.D., Mountain, G.S., Katz, M.E., Sugarman, P.J., Cramer, B.S., Christie-Blick, N., Pekar, S.F., 2005. The Phanerozoic Record of Global Sea-Level Change. Science 310 (5752), 1293–1298.

Miller, K.G., Browning, J.V., Schmelz, W.J., Kopp, R.E., Mountain, G.S., Wright, J.D., 2020. Cenozoic sea-level and cryospheric evolution from deep-sea geochemical and continental margin records. Science Advances 6 (20) eaaz1346.

Nelson, W.A., Sutherland, J.E., Farr, T.J., Hart, D.R., Neill, K.F., Kim, H.J., Yoon, H.S., 2015. Multi-gene phylogenetic analyses of New Zealand coralline algae: Corallinapetra Novaezelandiae gen. Et sp. nov. and recognition of the Hapalidiales Ord. Nov. J. Phycol. 51, 454–468.

Peña, V., Le Gall, L., Rösler, A., Payri, C.E., Braga, J.C., 2018. *Adeylithon bosencei* gen. Et sp. nov. (Corallinales, Rhodophyta): a new reef-building genus with anatomical affinities with the fossil *Aethesolithon*. J. Phycol. 55, 134–145.

Perrin, C., 2002. Tertiary: the emergence of modern reef ecosystems. In: Kiessling, W., Flügel, E., Golonka, J. (Eds.), Phanerozoic Reef Patterns: Society for Sedimentary Geology. Special Publication, pp. 587–621.

Perrin, C., Bosellini, F.R., 2012. Paleobiogeography of scleractinian reef corals: changing patterns during the Oligocene-Miocene climatic transition in the Mediterranean. Earth-Sci. Rev. 111 (1–2), 1–24.

Perrin, C., Bosence, D., Rosen, B., 1995. Quantitative approaches to palaeozonation and palaeobathymetry of corals and coralline algae in Cenozoic reefs. Geological Society London Special Publications 83 (1), 181–229.

Pomar, L., Hallock, P., 2007. Changes in coral-reef structure through the Miocene in the Mediterranean province_ Adaptive versus environmental influence. Geology 35 (10), 899–902.

Porzio, L., Buia, M.C., Lorenti, M., Vitale, E., Amitrano, C., Arena, C., 2018. Ecophysiological response of Jania rubens (Corallinaceae) to ocean acidification. Rendiconti Lincei-Scienze Fisiche E Naturali 29, 543–546.

Rasser, M.W., Piller, W.E., 2004. Crustose algal frameworks from the Eocene Alpine Foreland. Palaeogeogr. Palaeoclimatol. Palaeoecol. 206 (1), 21–39.

Rendina, F., Bouchet, P.J., Appolloni, L., Russo, G.F., Sandulli, R., Kolzenburg, R., Putra, A., Ragazzola, F., 2019. Physiological response of the coralline alga *Corallina officinalis* L. to both predicted long-term increases in temperature and short-term heatwave events. Marine Environmental Research 150, 104764.

Reolid, J., Betzler, C., Braga, J.C., Ludmann, T., Ling, A., Eberli, G.P., 2020. Facies and geometry of drowning steps in a Miocene carbonate platform (Maldives). Palaeogeogr. Palaeoclimatol. Palaeoecol. 538, 109455.

Retallack, G., 2007. Cenozoic Paleoclimate on Land in North America. The Journal of Geology 115 (3), 271–294.

Rösler, A., Pretković, V., Novak, V., Renema, W., Braga, J.C., 2015. Coralline algae from the Miocene mahakam delta (East Kalimantan, SE asia). Palaios 30, 83–93.

Rösler, A., Perfectti, F., Pena, V., Braga, J.C., Gabrielson, P., 2016. Phylogenetic relationships of corallinaceae (Corallinales, Rhodophyta): taxonomic implications for reef-building corallines. J. Phycol. 52 (3), 412–431.

Sane, E., Chiocci, F.L., Basso, D., Martorelli, E., 2016. Environmental factors controlling the distribution of rhodoliths: an integrated study based on seafloor sampling, ROV and side scan sonar data, offshore the W-Pontine Archipelago. Cont. Shelf Res. 129, 10–22.

Sarkar, S., 2017. Ecology of Coralline Red Algae and their Fossil Evidences from India. Thalassas An International Journal of Marine Sciences 33 (1), 1–14.

Schlager, W., 1981. The paradox of drowned reefs and carbonate platforms. Geol. Soc. Am. Bull. 92 (4), 197–211.

Schlager, W., 1999. Scaling of sedimentation rates and drowning of reefs and carbonate platforms. Geology 27 (2), 183–186.

Shao, L., Li, Q., Zhu, W., Zhang, D., Qiao, P., Liu, X., You, L., Cui, Y., Dong, X., 2017a. Neogene carbonate platform development in the NW South China Sea: Litho-, bio- and chemo-stratigraphic evidence. Mar. Geol. 385, 233–243.

Shao, L., Cui, Y., Qiao, P., Zhang, D., Liu, X., Zhang, C., 2017b. Sea-level changes and carbonate platform evolution of the Xisha Islands (South China Sea) since the early Miocene. Palaeogeography Palaeoclimatology Palaeoecology 485, 504-516.\.

Shevenell, A.E., Kennet, J.P., Lea, D.W., 2004. Middle Miocene Southern Ocean cooling and antarctic cryosphere expansion. Science 35, 1766–1770.

Steinthorsdottir, M., Coxall, H.K., de Boer, A.M., Huber, M., Barbolini, N., Bradshaw, C.D., Burls, N.J., Feakins, S.J., Gasson, E., Henderiks, J., Holbourn, A., Kiel, S., Kohn, M.J., Knorr, G., Kürschner, W.M., Lear, C., Liebrand, D., Lunt, D.J., Mörs, T., Pearson, P.N., Pound, M.J., Stoll, H., Strömberg, C.A.E., 2020. The Miocene: the Future of the past. Paleoceanography and Paleoclimatology e2020PA004037.

Steneck, R.S., 1986. The ecology of coralline algal crusts: convergent patterns and adaptative strategies. Annu. Rev. Ecol. Syst. 17 (1), 273–303.

Steneck, R.S., Macintyre, I.G., Reid, R.P., 1997. A unique algal ridge system in the Exuma Cays, Bahamas. Coral Reefs 16 (1), 29–37.

Veron, J.E.N., 2000. Corals of the World. Australian Institute of Marine Science, Townsville.

Wallace, C., 1999. Staghorn Corals of the World: A Revision of the Genus Acropora.

Wanamaker, A.D., Hetzinger, S., Halfar, J., 2011. Reconstructing mid- to high-latitude marine climate and ocean variability using bivalves, coralline algae, and marine sediment cores from the Northern Hemisphere. Palaeogeogr. Palaeoclimatol. Palaeoecol. 302 (1), 1–9.

Wang, P., 2009. Toward scientific breakthrough in the South China Sea. Journal of Tropical Oceanography 28 (3), 1–4.

Wang, P., Zhao, Q., Jian, Z., Cheng, X., Huang, W., Tian, J., Wang, J., Li, Q., Li, B., Su, X., 2003. The Deep Record since 30 Million Years in the South China Sea. Science Bulletin 48 (21), 2206–2215.

Wang, R., Yu, K., Jones, B., Wang, Y., Zhao, J., Feng, Y., Bian, L., Xu, S., Fan, T., Jiang, W., Zhang, Y., 2018. Evolution and development of Miocene "island dolostones" on Xisha Islands, South China Sea. Mar. Geol. 406, 142–158.

Webb, G.E., Nothdurft, L.D., Zhao, J., Opdyke, B., Price, G., 2016. Significance of shallow core transects for reef models and sea-level curves, Heron Reef, Great Barrier Reef. Sedimentology 63 (6), 1396–1424.

Webster, J.M., 2003. Coral variation in two deep drill cores: significance for the Pleistocene development of the Great Barrier Reef. Sediment. Geol. 159 (1), 61–80.

Williamson, C.J., Walker, R.H., Robba, L., Yesson, C., Brodie, J., 2015. Toward resolution of species diversity and distribution in the calcified red algal genera Corallina and Ellisolandia (Corallinales, Rhodophyta). Phycologia 54 (1), 2–11.

Woelkerling, W.J., 1988. Coralline Red Algae: an analysis of genera and subfamilies of nongeniculate Corallinaceae. In: British Museum (Natl. Hist.). London and Oxford University Press Oxford, pp. 1–268.

Woelkerling, W.J., Irvine, L.M., Harvey, A.S., 1993. Growth-forms in Non-geniculate Coralline Red Algae (Coralliinales, Rhodophyta). Aust. Syst. Bot. 6 (4), 277–293.

Wu, S., Zhu, W., Ma, Y., 2018. Vicissitude of Cenozoic carbonate platforms in the South China Sea: Sedimentation in semi-closed marginal seas. Marine Geology and Quaternary Geology 38 (6), 1–17.

Wu, F., Xie, X., Betzler, C., Zhu, W., Zhu, Y., Guo, L., Ma, Z., Bai, H., Ma, B., 2019. The impact of eustatic sea-level fluctuations, temperature variations and nutrient-level changes since the Pliocene on tropical carbonate platform (Xisha Islands, South China Sea). Palaeogeogr. Palaeoclimatol. Palaeoecol. 514, 373–385.

Xu, L., Liu, X., Sun, L., Yan, H., Liu, Y., Luo, Y., Huang, J., Wang, Y., 2010. Distribution of radionuclides in the guano sediments of Xisha Islands, South China Sea and its implication. J. Environ. Radioact. 101 (5), 362–368.

Yu, K., Zhao, J., 2009. Coral reefs. In: Wang, P., Li, Q. (Eds.), The South China Sea: Paleoceanography and Sedimentology. Springer Netherlands, Dordrecht, pp. 229–254.

Zachos, J., Pagani, M., Sloan, L., Thomas, E., Billups, K., 2001. Trends, rhythms, and aberrations in global climate 65 Ma to present. Science 292 (5517), 686–693.